

# Cyclam-based Chelators Bearing Phosphonated Pyridine Pendants for $^{64}\text{Cu}$ -PET Imaging : Synthesis, Physico-chemical Studies, Radiolabeling and Bioimaging.

Richard C. Knighton,<sup>a</sup> Thibault Troadec,<sup>\*a</sup> Valérie Mazan,<sup>c</sup> Patricia Le Saëc,<sup>b</sup> Séverine Marionneau-Lambot,<sup>b</sup> Thomas Le Bihan,<sup>a</sup> Nathalie Saffon-Merceron,<sup>d</sup> Nathalie Le Bris,<sup>a</sup> Michel Chérel,<sup>b</sup> Alain Faivre-Chauvet,<sup>b</sup> Mourad Elhabiri,<sup>c</sup> Loïc J. Charbonnière,<sup>e</sup> Raphaël Tripier<sup>\*a</sup>

<sup>a</sup> Univ. Brest, UMR CNRS 6521, 6 Avenue Victor Le Gorgeu, 29200 Brest, France.

\* E-mail: thibault.troadec@univ-brest.fr; raphael.tripier@univ-brest.fr

<sup>b</sup> Université de Nantes, CHRU de Nantes, Centre de Recherche en Cancérologie et Immunologie Nantes Angers (CRCINA), Unité INSERM 1232 – CNRS 6299, 8 quai Moncousu, BP 70721, 44007 Nantes Cedex, France.

<sup>c</sup> Université de Strasbourg, Université de Haute-Alsace, CNRS, UMR 7042-LIMA, Equipe de Chimie Bioorganique et Médicinale, ECPM, 25 rue Becquerel, Strasbourg 67087, France

<sup>d</sup> Institut de Chimie de Toulouse (FR 2599), 118 route de Narbonne, 31062 Toulouse Cedex 9, France.

<sup>e</sup> UMR 7178, Institut Pluridisciplinaire Hubert Curien, Université de Strasbourg, , ECPM, 25 rue Becquerel, 67087 Strasbourg Cedex 2, France.

**KEYWORDS :** Macrocyclic chemistry; Copper chelators ; PET imaging

**ABSTRACT:** Herein we present the preparation of two novel cyclam-based macrocycles (te1pyp and cb-te1pyp), bearing phosphonate-appended pyridine side-arms for the coordination of copper(II) ions in the context of  $^{64}\text{Cu}$  PET imaging. The two ligands have been prepared through conventional protection-alkylation sequences on cyclam, and their coordination properties have been thoroughly investigated. The corresponding copper complexes have been fully characterized in the solid-state (X-Ray diffraction analysis) and in solution (EPR and UV-Vis spectroscopies). Potentiometric studies, combined with spectrometry, have also allowed us to determine their thermodynamic stability constants, confirming their high affinity for copper(II) cations. The kinetic inertness of the complexes has also been verified by acid-assisted dissociation experiments, enabling their use in  $^{64}\text{Cu}$ -PET imaging in mice for the first time. Indeed, the two ligands could be quantitatively radiolabeled under mild conditions, and the resulting  $^{64}\text{Cu}$  complexes have demonstrated excellent stability in serum. PET imaging demonstrated a set of features emerging from the combination of picolinates and phosphonate units: high stability *in vivo*, fast clearance from the body via renal elimination, and most interestingly, very low fixation in the liver. The latter is in contrast with what was observed for monopicolinate cyclam (te1pa), that had a non-negligible accumulation in the liver, owing probably to its different charge and lipophilicity. These results thus pave the way for the use of such phosphonated pyridine chelators for *in vivo*  $^{64}\text{Cu}$ -PET imaging.

## INTRODUCTION

Positron Emission Tomography (PET) has emerged in the last decades as a key medical imaging modality, in the detection of physiological disorders and pathologies, and particularly in cancer detection. This technique relies on the injection of a radiopharmaceutical tracer, *i.e.* a molecule bearing a targeting moiety and labeled by a positron ( $\beta^+$ )-emitting radionuclide. The main benefits of PET, over other techniques, are its non-invasive character and very high sensitivity (nM concentration). In the clinic, the dominating tracer is  $^{18}\text{F}$ -Fluorodeoxyglucose ( $^{18}\text{F}$ -FDG), a glucose molecule labeled with  $\beta^+$ -emitting  $^{18}\text{F}$ , that relies on the Warburg effect in cancer cells, *i.e.* fast and high uptake of glucose to sustain their altered energy production mechanisms.<sup>1</sup> Although this tracer has a wide scope, it lacks specificity for the detection of some tumours, for instance in highly glucose-consuming organs such as the brain and liver.<sup>2</sup> In addition,  $^{18}\text{F}$  has a short half-life ( $t_{1/2} = 110$  min) that matches the fast glucose distribution *in vivo*, but is not appropriate for slower physiological mechanisms and labeling of biomolecules with longer biodistribution times (antibodies, pep-

tides). Thus, there is a high demand for new radiopharmaceuticals based on radionuclides having longer half-lives. In this context,  $^{64}\text{Cu}$  ( $t_{1/2} = 12.7$  h) is one nucleus of choice, and there is a strong need for chelating ligands that can accommodate copper(II) ions. To envisage an easy preparation of radiotracers and a safe use as PET tracers *in vivo*, a common set of characteristics is considered in the design of suitable ligands : i) high thermodynamic stability of the copper(II) complex (assessed by thermodynamic constants); ii) kinetic inertness, *i.e.* robustness towards transchelation and transmetallation (measured *in vivo* or by dissociation experiments in competitive media); iii) soft radiolabeling conditions to preserve the integrity of sensitive targeting units (antibodies in particular);<sup>3</sup> iv) good clearance from the body and the absence of undesired organ accumulation, which can have deleterious toxicological effects. To fulfil these attributes, nitrogen-based chelators have demonstrated their superior capabilities, and a large effort has been devoted in the last two decades to the design of functionalized polyazamacrocycles,<sup>4</sup> from 1,4,7,10-tetraazacyclododecane (cyclen) and 1,4,8,11-tetraazacyclotetradecane (cyclam) scaffolds in particular. Acetate coordinating pendant arms have long been used to increase the number of donor atoms

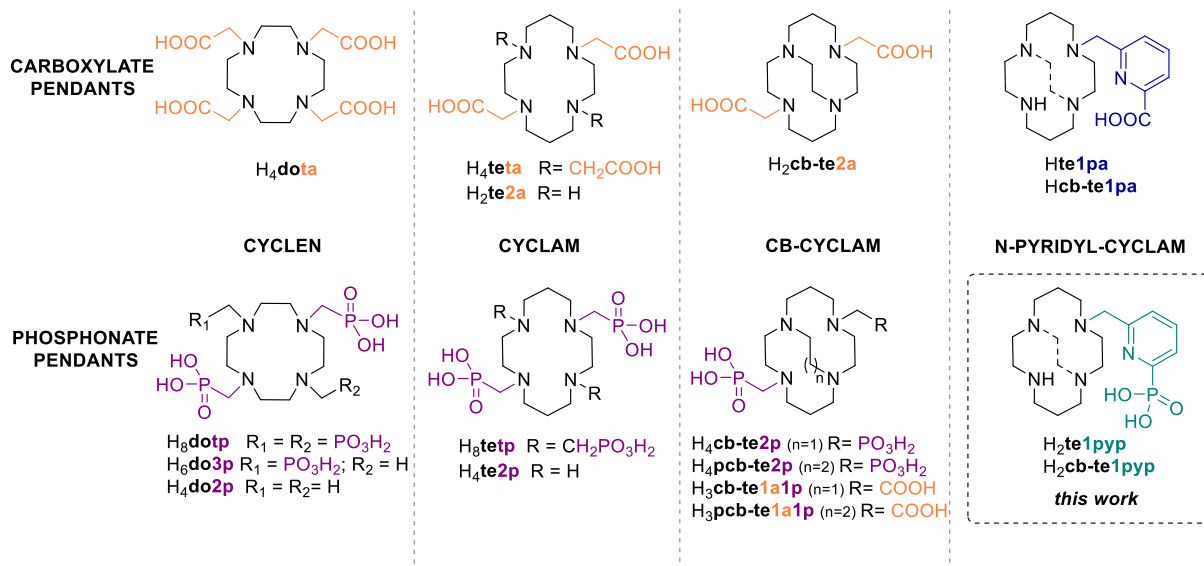


**Figure 1.** Copper(II) chelators discussed in this paper

and complex stability, and their characteristics are now well-known. More recently, phosphonate pendants have been introduced, and precise combinations of macrocyclic platform and side-arms have allowed a fine control of the chelators properties, following a few clear trends.

Owing to its commercial availability and coordination properties towards a wide range of metallic cations, 1,4,7,10-tetraazacyclododecane-1,4,7,10-tetraacetic acid (**H<sub>4</sub>dota**, **Figure 1**) has been extensively studied and its analogues are still used in preclinical investigations for copper complexation and PET applications.<sup>5</sup> However, its lack of selectivity for copper and metal dissociation occurring in competitive media are detrimental for human *in vivo* use.<sup>6</sup> When moving to larger 1,4,8,11-tetraazacyclotetradecane-1,4,7,10-tetraacetic acid (**H<sub>4</sub>teta**) congener, a strong increase in copper selectivity is observed. Indeed, **teta**<sup>4-</sup> exhibits a stability constant with copper similar to **dota**<sup>4-</sup> (log  $K_{CuL}$  = 21.1 and 22.2 respectively), but a marked preference for copper(II) over zinc(II) (log  $K_{ZnL}$  = 17.5 and 21.1 respectively),<sup>7</sup> a competitive biologically-abundant cation. However, the kinetic inertness of the complexes is still below requirements.<sup>8</sup> Nevertheless, studies on **H<sub>2</sub>te2a**, bearing only two acetate units, have clearly demonstrated that reducing the number of coordinating pendants to match copper(II) preferred coordinating numbers (5-6) drastically improves the kinetic inertness of the corresponding copper complexes ( $t_{1/2}$  = 92 h for **H<sub>2</sub>te2a** ligand vs. 4 h for **H<sub>4</sub>teta** in 5 M HCl at 50 °C).<sup>9</sup> The cross-bridged analogue **H<sub>2</sub>cb-te2a**, exhibiting an extra ethylene linkage between two *trans*-nitrogen atoms, also demonstrates high inertness attributed to the rigidity of its pre-organized cavity.<sup>10</sup> However, complexation kinetics are dramatically reduced with such architectures, and harsh conditions are necessary for quantitative radiolabeling with <sup>64</sup>Cu ( $T > 75^\circ\text{C}$  and  $t > 1\text{h}$  for **H<sub>2</sub>cb-te2a**<sup>11,12</sup> vs. 5 min at 30 °C for **H<sub>2</sub>te2a**).<sup>9</sup> In this context, some of us have recently prepared picolinate-functionalized cyclam and cross-bridged cyclam **Hte1pa** and **Hcb-te1pa**, presenting an ideal combination of thermodynamic stabil-

ity, copper selectivity, inertness and fast complexation kinetics.<sup>13-15</sup> To access *in vivo* applications while retaining **Hte1pa** coordination properties, the cyclam scaffold was derivatized to design a bifunctional analogue, that was successfully grafted on antibodies for immuno-PET imaging on mice.<sup>16-18</sup>

In addition to this scaffold tuning, methylenephosphonate side-arms have also attracted attention and facilitate modulation of the ligand coordination properties. As a general trend, compared to carboxylates, they have been shown to provide faster copper(II) complexation kinetics, but at the detriment of inertness. These features were exemplified on cyclen derivatives with a systematic series of **H<sub>4</sub>dota** analogues where up to four acetate pendants were replaced by methylphosphonates.<sup>19</sup> The same behaviour is observed on cyclam scaffolds, with **H<sub>4</sub>teta** and **H<sub>2</sub>te2a** complexes showing much higher inertness (4 and 92 h in 5 M HCl at 50 °C respectively)<sup>9</sup> than their phosphonated counterparts **H<sub>8</sub>tetp** and **H<sub>4</sub>te2p** (19 min in 1 M HClO<sub>4</sub> at 25 °C for **te2p**).<sup>20,21</sup> Finally, as previously demonstrated for the carboxylate parents, addition of an ethylene- or propylene-cross-bridged in **H<sub>4</sub>cb-te2p** and **H<sub>4</sub>pcb-te2p** leads to more inert complexes,<sup>10,22</sup> even if lower in magnitude than the corresponding **H<sub>2</sub>cb-te2a** and **H<sub>2</sub>pcb-te2a**.<sup>10,23</sup> However, faster complexation kinetics and radiolabeling are still observed for the phosphonated macrocycles.

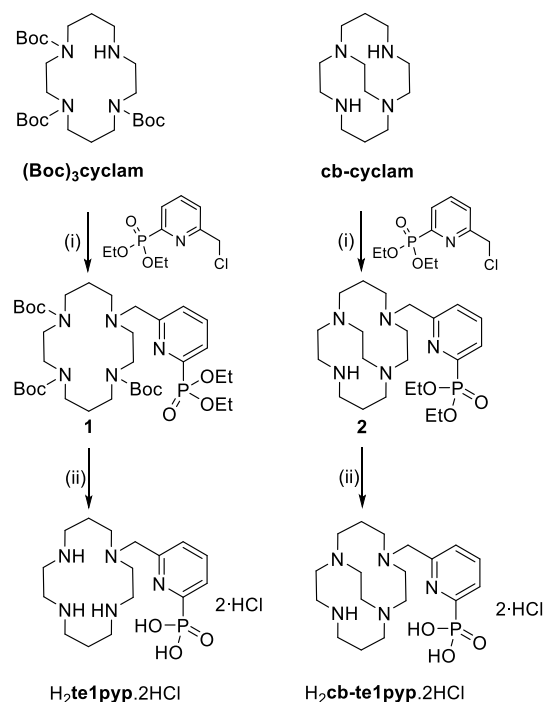
Finally, the nature and charge of the side-arms strongly affects the biodistribution of the injected complexes. Although both series generally show fast blood clearance due to the small size of the complexes, phosphonate-appended complexes typically display renal elimination, whereas hepatic accumulation can be observed with the carboxylate congeners. This is due in some cases to free copper resulting from complex dissociation, as demonstrated for **H<sub>4</sub>dota** and **H<sub>4</sub>teta** ligands,<sup>15,24</sup> or simply to the hepatic affinity of the molecule in the case of perfectly inert complexes.<sup>17</sup> The capacity of phosphonates to reduce this behaviour was clearly demonstrated with phosphonate and mixed acetate/methylenephosphonate ligands **H<sub>4</sub>(p)cb-te2p** and **H<sub>3</sub>(p)cb-**

**te1a1p** when compared to the  $H_2cb\text{-te2a}$  analogue.<sup>10,23,25–27</sup> However, increasing the number of phosphonate groups to three or four is detrimental with accumulation increasing in both the liver and kidneys.<sup>28</sup>

Based on these trends, we sought to develop  $H_2te1pyp$  and  $H_2cb\text{-te1pyp}$ , cyclam and cross-bridged cyclam macrocycles mono-functionalized with a 2-phosphorylpyridyl side-arm, a coordinating unit that has been recently used by our groups for lanthanide coordination.<sup>29–31</sup> The two novel ligands are expected to combine the stability and inertness of their parent **te1pa** and **cb-te1pa** complexes with reduced hepatic accumulation owing to the replacement of the carboxylate by a phosphonate moiety. Herein, we present a thorough description of the synthesis, solution and solid-state studies, physico-chemical properties, radiolabeling and PET imaging ability of these two novel copper(II) chelators.

## RESULTS AND DISCUSSION

**Synthesis of ligands, complexes and solid-state structures.** The synthetic protocol for the preparation of the ligands is depicted in **Scheme 1** and full experimental details can be found in the experimental section (Section 2).



**Scheme 1.** Synthetic protocol for the preparation of the ligands;  $H_2te1pyp$  and  $H_2cb\text{-te1pyp}$ ; (i)  $K_2CO_3$ , MeCN, RT, 36 hr (**1** 58%; **2**·HCl 84%) (ii) 6 M  $HCl_{(aq)}$ , 100°C, 36 hr ( $H_2te1pyp$  89%;  $H_2cb\text{-te1pyp}$  60%)

The target monofunctionalized cyclam ligands  $H_2te1pyp$  and  $H_2cb\text{-te1pyp}$  were synthesized according to an operationally simple procedure. The tris(*tert*-butoxycarbonyl)-protected cyclam precursor<sup>32</sup> was alkylated with diethyl (6-(chloromethyl)pyridin-2-yl)phosphonate<sup>29</sup> in anhydrous acetonitrile under basic conditions to obtain the tri-protected intermediate **1** in 58% yield. The ligand  $H_2te1pyp$  was obtained *via* simultaneous cleavage of the acid sensitive

Boc and ester protecting groups using aqueous HCl yielding 89% of isolated compound after recrystallization. The corresponding cross-bridged intermediate **2** was obtained in 84% yield following a controlled statistical alkylation. Again, deprotection and recrystallization furnished the target  $H_2cb\text{-te1pyp}$  in good yield (60%).

The novel ligands  $H_2te1pyp$  and  $H_2cb\text{-te1pyp}$  were investigated for the ability to chelate  $Cu^{2+}$  ions. Complexation of the metal as the perchlorate salt was achieved in  $H_2O$  (pH = 6.5 – 7.0), obtaining the paramagnetic complexes  $[Cu(\text{te1pyp})H][ClO_4]$  (88%) and  $[Cu(\text{cb-te1pyp})H][ClO_4]$  (38%) after acidification (pH = 3.5 – 4.0) and purification by  $C_{18}$  chromatography. Complexes gave characteristic ESI-HRMS peaks and their purity was confirmed by analytical HPLC-MS (See ESI, **Section 2.2.2**). The diamagnetic zinc(II) congeners were prepared *via* an analogous procedure ( $[Zn(\text{te1pyp})H][ClO_4]$ , 57%;  $[Zn(\text{cb-te1pyp})H][ClO_4]$ , 60%), and were fully characterized by  $^1H$ ,  $^{13}C$ ,  $^{31}P$  NMR and ESI-HRMS (See ESI, **Section 2.2.1**).

Slow evaporation of concentrated  $H_2O$  solutions of the copper complexes yielded crystals suitable for analysis by single crystal X-ray diffraction (See ESI, **Section 3** for full

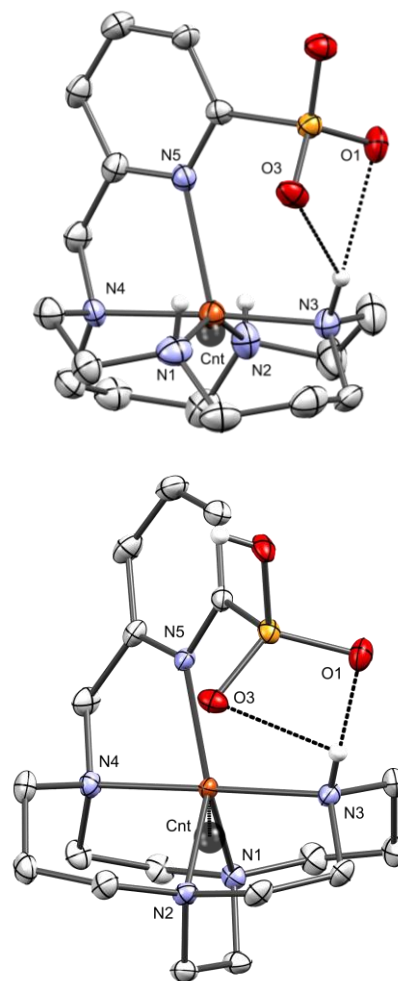


**Figure 2:** Single crystal X-rays structures of  $[Cu(\text{te1pyp})]$  (top) and  $[Cu(\text{cb-te1pyp})H]^+$  (bottom) (Ellipsoids are plotted at 30% and 50% respectively, non-heteroatoms hydrogen bonds, solvents and anions are omitted for clarity; Cnt = N1-N2-N3-N4 centroid).

**Table 1: Selected bond lengths for novel Copper(II) complexes (Å)**

	Cu1-N1	Cu1-N2	Cu1-N3	Cu1-N4	Cu1-N5	N3-O1	N3-O3	$\tau$
<b>[Cu(te1pyp)]</b>	2.035(4)	2.038(5)	1.984(5)	2.054(5)	2.345(4)	3.131(6)	3.125(6)	0.427
<b>[Cu(cb-te1pyp)H]<sup>+</sup></b>	2.143(2)	2.082(2)	1.996(2)	2.006(2)	2.077(2)	2.867(2)	3.470(2)	0.619

details). Both complexes crystallize in the monoclinic  $P2_1/c$  space group, and reveal the extended Cu1-O1/3 distances and thus 5-coordinate ( $N_5$ ) complexes (**Table 1**). Comparing the native and cross-bridged variant, [Cu(**te1pyp**)] shows shortened cyclam metal-nitrogen distances and a lengthened metal-pyridine bond (largest  $\Delta A = 0.361$  Å), whereas [Cu(**cb-te1pyp**)H]<sup>+</sup> exhibits broadly similar Cu-N bond lengths (largest  $\Delta A = 0.147$  Å). This disparity is reflected in the coordination sphere of each complex; the calculated values are  $\tau = 0.43$  and  $\tau = 0.62$  for [Cu(**te1pyp**)] and [Cu(**cb-te1pyp**)H]<sup>+</sup> respectively, indicating a tendency away from the square pyramidal geometry of [Cu(**te1pyp**)] towards a trigonal bipyramidal geometry in [Cu(**cb-te1pyp**)H]<sup>+</sup>.<sup>33</sup> The difference in metal coordination geometry is mirrored in the lateral displacement of the copper ion away from the central cyclam cavity in the cross-bridged analogue (Cn<sub>N1-N2-N3-N4</sub>-Cu1: [Cu(**te1pyp**)] = 0.296(2) Å; [Cu(**cb-te1pyp**)H]<sup>+</sup> = 0.771(1) Å). Despite the absence of phosphonate oxygen coordination, both structures reveal supplementary stabilizing hydrogen bonding between the phosphonate oxygen atoms and the azamacrocyclic NH atoms ([Cu(**te1pyp**)]: N3-O1 = 3.131(6) Å, N3-O3 = 3.125(6) Å; [Cu(**cb-te1pyp**)H]<sup>+</sup>: N3-O1 = 2.867(2) Å, N3-O3 = 3.470(2) Å), which encloses the central copper ion and increases the stability/inertness of the complexes (*vide infra*), as in the case of previously described picolinate moiety.<sup>13</sup>

**Solution-state properties – Zn(II) complexes.** The paramagnetic character of the copper(II) complexes precludes their characterisation using NMR analysis. Consequently, the diamagnetic zinc(II) complexes were employed as a surrogate for elucidation of the solution-state structural properties of the novel complexes. NMR spectra were recorded – in an analogous fashion to the ligands – in aqueous solutions (D<sub>2</sub>O, pD ≈ 7.0, 400 MHz, 298 K). At this pD, by analogy with their corresponding Cu<sup>2+</sup> counterparts (*vide infra*), these complexes are neutral in solution, both phosphonate oxygen atoms being deprotonated and compensating the Zn<sup>2+</sup> charge. As a general comparison both [Zn(**te1pyp**)] and its cross-bridged congener [Zn(**cb-te1pyp**)] exhibit significant perturbations of the <sup>1</sup>H NMR spectra compared to their respective free ligands upon complexation of the electropositive zinc(II) metal cation, notably for the diastereotopic methylene CH<sub>2</sub> protons corresponding to the 2-phosphorylpyridine arm. The solution-state analysis by <sup>1</sup>H NMR also shows that the cross-bridged [Zn(**cb-te1pyp**)] complex exhibits *C*<sub>1</sub> symmetry in solution – mirroring the solid-state copper geometry – consistent with slow interconversion on the <sup>1</sup>H NMR timescale. The symmetry is typified by diastereotopic resonances ( $\delta = 4.63$  and 3.74 ppm) of the methylenic 6-phosphonated pyridine moiety. The corresponding [Zn(**te1pyp**)] complex again presents a *pseudo-C*<sub>1</sub> symmetry but exhibits more dynamic behaviour with several methylenic resonances approaching the fast-exchange limit

(400 MHz, 298 K). This can be rationalised by the less rigid structure of the unfunctionalized complex in comparison to the rigid geometry imposed by the cross-bridged appendage, which reduce degrees of freedom of the cyclam backbone.

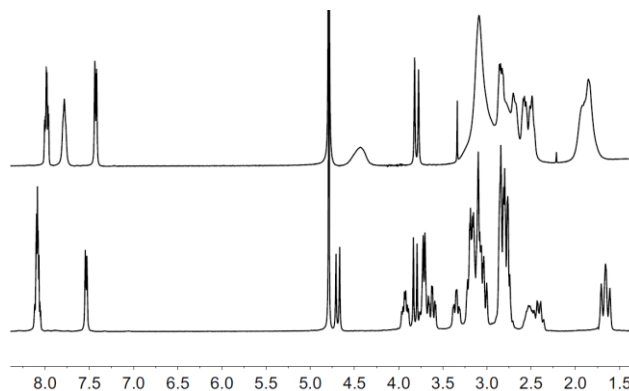


**Figure 3.** <sup>1</sup>H NMR spectra (D<sub>2</sub>O, pD ≈ 7.0, 400 MHz, 298 K) of zinc(II) complexes [Zn(**te1pyp**)] (top) and [Zn(**cb-te1pyp**)] (bottom)

**EPR analysis.** The spin-state of the copper(II) complexes was investigated by electron paramagnetic resonance (EPR) spectroscopy. Complexes were studied in frozen glass (1:1 H<sub>2</sub>O/DMF, 150 K, X-band) and the EPR spectra of the complexes [Cu(**te1pyp**)] and [Cu(**cb-te1pyp**)] were

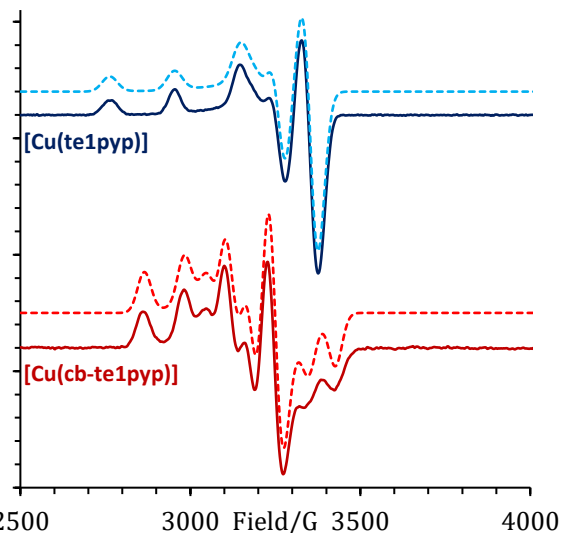


**Figure 4.** X-band EPR spectrum of copper(II) complexes [Cu(**te1pyp**)] (– experimental; - - - simulation) and [Cu(**cb-te1pyp**)] (– experimental; - - - simulation) recorded in frozen aqueous solution (1:1 DMF/H<sub>2</sub>O, 1.0 mM; 150K)

recorded as their neutral deprotonated forms; simulation of the spectra confirmed the presence of only one observable paramagnetic species (**Figure 4**). Both spectra exhibit typical resonances corresponding to the paramagnetic copper(II) ion with elongated axial symmetry,<sup>34–37</sup> although the spectra indicate a significant difference in copper(II) geometry for each respective complex. The EPR spectra show only characteristic copper hyperfine splitting, with observation of hyperfine coupling  $g_z$  component for three of the maxima at low-field (**Table 2**), the other being obscured by the second-order portion of the spectra. Additionally, as expected, no superhyperfine coupling was observed to proximal spin-active <sup>14</sup>N or <sup>31</sup>P nuclei of the cyclam backbone or phosphonated appendage, indicating the unpaired electron is confined and located exclusively on the copper(II) ion. Simulation of the spectra indicate distorted axial symmetry with three distinct principal values for the  $g$  parameter for both complexes. In the case of the less rigid complex [Cu(**te1pyp**)], the geometry lies closer to an undistorted axial symmetry ( $g_x \approx g_y < g_z$ ), while the observation that  $\{g_z > (g_x + g_y)/2\}$  and the smallest  $g \geq 2.03$ , exemplifies mononuclear copper(II) complexes in a rhombic symmetry with axial elongation and a  $d_{x^2-y^2}$  ground state.<sup>38–40</sup> In complexes of this type this is most accurately described as square pyramidal geometry, in good agreement with the solid-state structure (*vide supra*). This contrasts with the cross-bridged complex [Cu(**cb-te1pyp**)] which displays inverse parameters ( $g_x < g_y < g_z$ ) with a similar  $\Delta g$  between each cartesian coordinate value. These properties point towards a  $d_{z^2}$  ground state and thus a trigonal prismatic geometry. This observation corroborates well with the  $\tau$  values calculated for both [Cu(**te1pyp**)] and [Cu(**cb-te1pyp**)H]<sup>+</sup> in the single-crystal X-ray studies (*vide supra*). It can thus be concluded that, qualitatively, both complexes retain their coordination geometry between the solid- and solution-state.

**Table 2. Spectroscopic Parameters for Copper(II) complexes [Cu(**te1pyp**)] and [Cu(**cb-te1pyp**)] in aqueous solution (UV-vis measurements performed in H<sub>2</sub>O (293 K); EPR measurements performed in 1:1 H<sub>2</sub>O/DMF glass (1.0 mM, 150 K;  $A_i$  values quoted in 10<sup>-4</sup> cm<sup>-1</sup>)**

UV-vis			
[Cu( <b>te1pyp</b> )]	215 (4000), 274 (4300), 604 (200)		
[Cu( <b>cb-te1pyp</b> )]	229 (3500), 286 (4000), 555 (200), 937 (135)		
EPR			
	$g_x$	$g_y$	$g_z$
[Cu( <b>te1pyp</b> )]	2.049	2.031	2.181
[Cu( <b>cb-te1pyp</b> )]	2.185	2.105	2.005

**Acid-Base Properties.** Detailed interpretation of the physico-chemical data on the cupric complexes with **te1pyp**<sup>2-</sup> and **cb-te1pyp**<sup>2-</sup> requires the characterization of the protonation pattern of the ligands, at least in the pH range relevant to the targeted application (*i.e.*, PET imaging). We therefore investigated the acido-basic properties of the ligands in the pH range 2.0–11.5 by various techniques. Both **te1pyp**<sup>2-</sup> and **cb-te1pyp**<sup>2-</sup> display four cyclam amino functions, one pyridine and one phosphonate –PO<sub>3</sub><sup>2-</sup> moiety. Potentiometric measurements (1–2 mM solutions)

were first performed to characterize and quantify the majority of the seven protonation sites (ESI, Figures S1 and S3). Some of the protonation constants were indeed difficult to measure with high accuracy due to their low values ( $\log K^H \ll 2$ , *vide infra*). **Table 3** summarizes the data resulting from the statistical processing of the potentiometric data. Three protonation constants were determined for **te1pyp**<sup>2-</sup>, while only two  $pK_a$  values were accurately calculated for its cross-bridged analogue **cb-te1pyp**<sup>2-</sup>. For **te1pyp**<sup>2-</sup>, the two highest protonation constants ( $\log K_{1H} = 11.04(3)$  and  $\log K_{2H} = 10.30(3)$ ) were attributed to two secondary amines of the tetraazamacrocycle, in excellent agreement with related systems such as **cyclam** ( $\log K_{11} = 11.29$  and  $\log K_{12} = 10.19(1)$ ,<sup>41</sup>  $\log K_{11} = 11.585(5)$  and  $\log K_{12} = 10.624(4)$ <sup>42</sup>) or **te1pa**<sup>-</sup> ( $\log K_{11} = 11.55(1)$  and  $\log K_{12} = 10.11(1)$ )<sup>13</sup>. The  $pK_a$  values of the two remaining amines were estimated to be significantly lower than 2.5 (*e.g.*,  $\log K_{13} = 2.41^{42}/1.91^{41}$  and  $\log K_{14} = 1.61$  for **cyclam**<sup>41,42</sup>) as the consequence of electrostatic repulsion from ammonium cations.

In the case of cross-bridged scaffolds, proton sponge character (*i.e.*, stabilization of the first proton by intramolecular hydrogen bonds and solvation effects) has been well-described in the literature,<sup>43–47</sup> resulting in very high  $pK_a$  values for the first protonation equilibrium of the tetraazamacrocycle. The cross-bridged analogue **cb-te1pyp**<sup>2-</sup> does not stand out from this trend as evidenced by the inability to determine the first protonation constant of the cyclam scaffold. Only the second protonation constant ( $\log K_{12} = 11.38(3)$ ) was accurately evaluated and its value was found to be one order of magnitude higher than those determined for closely related derivatives (**cb-cyclam**,  $\log K_{12} = 10.20^{27}$  and **cb-te1pa**<sup>-</sup>;  $\log K_{12} = 10.13^{14}$ ) suggesting additional stabilization by the phosphonate unit. Similarly to **te1pyp**<sup>2-</sup>, the  $pK_a$  values of the two other amino function of the tetraazamacrocycle were estimated to be  $\ll 2.5$ .

The following protonation constant of **te1pyp**<sup>2-</sup> ( $\log K_{13} = 5.85(5)$ ) and **cb-te1pyp**<sup>2-</sup> ( $\log K_{13} = 5.41(2)$ ) was assigned to the first protonation constant of the phosphonate –PO<sub>3</sub><sup>2-</sup> units (*i.e.*,  $\text{RPO}_3^{2-} + \text{H}^+ \rightleftharpoons \text{RPO}_3\text{H}^-$ ). Interestingly, these  $pK$  values are almost one order of magnitude lower than observed for other phosphonate functionalities,<sup>48</sup> even in the case of pyridylphosphonic acids.<sup>31,49</sup> The second protonation constant of the monoprotonated phosphonate groups (*i.e.*,  $\text{RPO}_3\text{H}^- + \text{H}^+ \rightleftharpoons \text{RPO}_3\text{H}_2$ ) was estimated to be very low ( $\ll 2$ ). For **te1pyp**<sup>2-</sup> or **cb-te1pyp**<sup>2-</sup>, the protonation constant of the pyridyl unit cannot be assessed and their  $\log K_{14}$  values were estimated to be  $\ll 2$ . This is consistent with the values determined for the closely related carboxylate analogues **te1pa**<sup>-</sup> ( $\log K_{14} = 1.7(1)$ )<sup>13</sup> and **cb-te1pa**<sup>-</sup> ( $\log K_{14}$  not determined)<sup>14</sup>. According to the protonation diagrams established in this work, the two ligands predominate as neutral zwitterionic species (H<sub>2</sub>**te1pyp** and H<sub>2</sub>**cb-te1pyp** respectively) at pH 7.0 (**Figure 6**), with the tetraazamacroyclic scaffold bearing two positive charges, and the phosphonate unit being under its dianionic form.

**Table 3. Protonation constants ( $\log K_{\text{th}}$ )<sup>a</sup> for ligands **te1pyp** and **cb-te1pyp** compared to literature data reported for closely related systems.**

Equilibrium / Constant	$\log K_{\text{th}} (\pm 3\sigma)$						
	<b>te1pyp</b> <sup>2-</sup>	<b>cb-te1pyp</b> <sup>2-</sup>	<b>te1pa</b> <sup>-</sup> ref. <sup>13</sup>	<b>cb-te1pa</b> <sup>-</sup> ref. <sup>14</sup>	<b>cyclam</b> ref. <sup>41</sup>	<b>cb-cyclam</b> ref. <sup>27</sup>	<b>te2p</b> <sup>2-</sup> ref. <sup>42</sup>
$L + H \rightleftharpoons LH$ $\log K_{11}$	11.04(3) <sup>b,e</sup>	g	11.55(1) <sup>e</sup>	g	11.29 <sup>e</sup>	12.42 <sup>e</sup>	
$LH + H \rightleftharpoons LH_2$ $\log K_{12}$	10.30(3) <sup>b,e</sup>	11.38(3) <sup>b,e</sup> 11.3(6) <sup>c,e</sup>	10.11(1) <sup>e</sup>	10.13(5) <sup>e</sup>	10.19 <sup>e</sup>	10.20 <sup>e</sup>	
Mean.( $\log K_{11}$ ; $\log K_{12}$ )	10.98(6) <sup>c,e</sup>	na					
$L + 2H \rightleftharpoons LH_2$ $\log \beta_{12}$							26.41 <sup>e</sup>
$LH_2 + H \rightleftharpoons LH_3$ $\log K_{13}$	5.85(5) <sup>b,d</sup> 5.93(6) <sup>c,d</sup>	5.41(2) <sup>b,d</sup> 5.3(6) <sup>c,d</sup>	2.71(1) <sup>f</sup>	2.43(7) <sup>f</sup>	1.61 <sup>e</sup>		6.78 <sup>d</sup>
$LH_3 + H \rightleftharpoons LH_4$ $\log K_{14}$			1.7(1) <sup>e</sup>		1.91 <sup>e</sup>		5.36 <sup>d</sup>
$LH_2 + 2H \rightleftharpoons LH_4$ $\log K_{13} + \log K_{14}$						1.39 <sup>e</sup>	
$LH_4 + H \rightleftharpoons LH_5$ $\log K_{15}$							1.15

Further information was obtained from absorption *versus* pH titrations ( $\lambda_{\text{abs}} = 220 - 400$  nm, ESI, Figures S2 and S4). For **te1pyp**<sup>2-</sup> or **cb-te1pyp**<sup>2-</sup>, marked spectral variations were observed in neutral to acidic pH range (and to lesser extend under basic conditions) in line with the (de)protonation of the phosphonate-pyridine substituent (*i.e.*, pyridine is the main chromophore with  $\pi-\pi^*$  transitions centered at 265-270 nm and  $\epsilon \approx 10^4$  M<sup>-1</sup> cm<sup>-1</sup>). For both chelators, the statistical processing of the spectrophotometric

and potentiometric data allowed accurate evaluation of two protonation constants. The most basic protonation constant (*i.e.*, mean value between  $\log K_{11}$  and  $\log K_{12}$ ; significant spectral variation at 225 nm related to the amine n- $\sigma^*$  transitions) of **te1pyp**<sup>2-</sup> was easily assigned to two of the cyclam ionizable sites. For **cb-te1pyp**<sup>2-</sup>, the protonation constant determined ( $\log K_{12} = 11.3(6)$ ) most likely corresponds to the second protonation equilibrium and is in excellent agreement with that determined by potentiometry ( $\log K_{12} = 11.38(3)$ ). The second protonation constant measured for **te1pyp**<sup>2-</sup> ( $\log K_{12} = 5.96(6)$ ) or **cb-te1pyp**<sup>2-</sup> ( $\log K_{12} = 5.3(6)$ ) can be attributed to the phosphonate unit and its value corresponds very well to that determined previously (**te1pyp**<sup>2-</sup>,  $\log K_{12} = 5.85(5)$  and **cb-te1pyp**<sup>2-</sup>,  $\log K_{12} = 5.41(2)$ ). The protonation of these phosphonate units therefore influences the pyridine transitions, as indicated by the significant spectral variations measured at neutral to weakly acidic pH at 270 nm.

**Cu(II) coordination properties of te1pyp and cb-te1pyp.** The stability constants of the cupric complexes with **te1pyp**<sup>2-</sup> and **cb-te1pyp**<sup>2-</sup> were first assessed by potentiometric means (ESI, Figures S5-S8). The statistical analyses of the potentiometric data allowed the determination of the resulting stability constants that are gathered in Table 3. Only the expected monocupric monochelates were evidenced in agreement with the preliminary LC-ESI-MS studies (see ESI, Section 5). For **te1pyp**<sup>2-</sup>, the stability constant was too high to be determined directly and accurately. To overcome this problem, the formal stability constant for the formation of [Cu(**te1pyp**)] was evaluated from a UV-Vis. absorption spectrophotometric titration carried out under acidic conditions (pH = 1.53, ESI, Figure S7) to ensure sufficient destabilization of the metal complex. This allowed access to the conditional stability constant ( $\log K_{\text{Cu-te1pyp}}^* = 5.8(4)$  at pH 1.53; the asterisk designates the apparent conditions of pH). The formal stability constant of the [Cu(**te1pyp**)] complex ( $\log K_{\text{Cu-te1pyp}} = 25.49$ ) was then extrapolated from the conditional stability constant measured at pH 1.53, the protonation constants of the free ligand **te1pyp**<sup>2-</sup> and of the copper(II) complex (Table 3 and Table 4).<sup>50</sup> [Cu(**te1pyp**)] complex was also shown to undergo a protonation equilibrium ( $\log K_{\text{Cu-te1pypH}} = 5.12(2)$ ) under weakly acidic conditions that was attributed to one of the

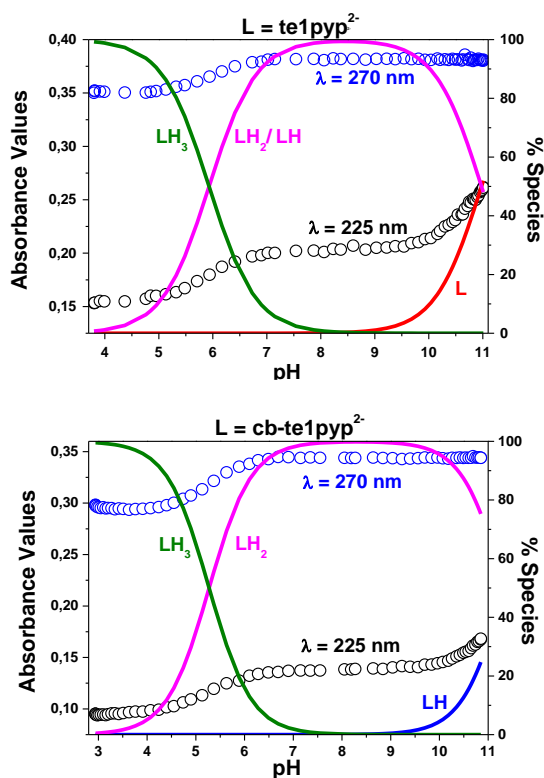


**Figure 6.** Distribution diagrams of the protonated species of **te1pyp**<sup>2-</sup> (top) and **cb-te1pyp**<sup>2-</sup> (bottom) in solution from absorption *versus* pH data, compared to the variation of the absorbance at 270 nm and 225 nm as a function of the pH

**Table 4. Logarithms of the global ( $\log \beta_{\text{mlh}}$ ) and successive ( $\log K_{\text{mlh}}$ ) stability and protonation constants for the cupric complexes with **te1pyp**<sup>2-</sup> and **cb-te1pyp**<sup>2-</sup> compared to literature data reported for closely related systems.<sup>a</sup>**

Equilibrium	Constant	<b>te1pyp</b> <sup>2-</sup>	<b>cb-te1pyp</b> <sup>2-</sup>	<b>te1pa</b> <sup>-</sup>	<b>cb-te1pa</b> <sup>-</sup>	cyclam	cb-cyclam	<b>te2p</b> <sup>2-</sup>
				ref. <sup>13</sup>	ref. <sup>14</sup>			ref. <sup>42</sup>
<b><math>\log \beta_{\text{mlh}} (\pm 3\sigma)</math></b>								
Cu + L $\rightleftharpoons$ CuL	$\log \beta_{110}$	25.49 <sup>c</sup>	g	25.5	g	26.5(1) <sup>52</sup> 28.1 <sup>53</sup> 27.2 <sup>54</sup>	27.1 <sup>11</sup>	25.4
Cu + L + H $\rightleftharpoons$ CuLH	$\log \beta_{111}$	30.78(2) <sup>b,e</sup>		27.67 <sup>f</sup>				32.45
Cu + L + 2H $\rightleftharpoons$ CuLH <sub>2</sub>	$\log \beta_{112}$							37.55
Cu + L $\rightleftharpoons$ CuL(OH) + H	$\log \beta_{11-1}$			14.35				
Cu + HL $\rightleftharpoons$ CuL + H	$\log \beta_{110} - \log \beta_{101}$	13.03(4) <sup>b</sup>		-	11.00(5)			
Cu + HL $\rightleftharpoons$ CuLH	$\log \beta_{110} - \log \beta_{11} - \log K_{111}$	18.32(4) <sup>b,e</sup>						
Cu + HL $\rightleftharpoons$ CuL(OH) + 2H	$\log \beta_{110} + \log \beta_{11-1}$			-	0.95(9)			
<b><math>\log K_{\text{mlh}} (\pm 3\sigma)</math></b>								
CuL + H $\rightleftharpoons$ CuLH	$\log K_{111}$	5.12(2) <sup>b,e</sup> 5.8(2) <sup>d,e</sup>	5.29(4) <sup>b,e</sup> 5.4(7) <sup>d,e</sup>	2.17 <sup>f</sup>				7.05
CuLH + H $\rightleftharpoons$ CuLH <sub>2</sub>	$\log K_{112}$							5.1
CuL(OH) + H $\rightleftharpoons$ CuL	$\log K_{11-1}$	-		11.15	10.05			
<b>pCu</b>								
		19.89	17.40 <sup>i</sup>	19.59	16.62 <sup>i</sup>	20.04 <sup>13</sup>	20.23 <sup>11</sup>	14.81

<sup>a</sup> Values in parentheses are standard deviations ( $3\sigma$ ) in the last significant digit.  $I = 0.1$  M (NaCl);  $T = 25.0(2)$ .  $\beta_{\text{mlh}} = [\text{Cu}_m\text{L}_m\text{H}_h]/[\text{Cu}]^m[\text{L}]^m[\text{H}]^h$ . Charges omitted for the sake of clarity. <sup>b</sup> potentiometry. <sup>c</sup> Absorption titration at pH 1.53. <sup>d</sup> Absorption versus pH titration. <sup>e</sup> phosphonate units. <sup>f</sup> carboxylate units. na = not applicable. <sup>g</sup> Too high to be determined. <sup>h</sup>  $\text{pCu} = -\log[\text{Cu}^{2+}]_{\text{free}}$  for  $[\text{L}] = 10^{-5}$  M,  $[\text{Cu}] = 10^{-6}$  M and pH 7.4, ref<sup>55</sup>. The pCu is a measure of the equilibrium concentrations of free  $\text{Cu}^{2+}$  ion. Its value describes the complexing efficiency of the chelating agents and takes into account the difference in basicity of the ligands and stoichiometry of the cupric complexes.  $\log K_{\text{Cu(OH)}^+} = -6.29$  and  $\log K_{\text{Cu(OH)}_2} = -13.1$  ref. <sup>56</sup>. <sup>i</sup> calculated with  $\log K_{11}$  estimated at 13.

three oxygen atom from the phosphonate moiety, the two other oxygen atoms being involved in the stabilization of the cupric complex through hydrogen bonding with the tetraazamacrocyle as shown by the solid-state structure (**Figure 2**). The slight diminution of this protonation constant with respect to the free ligand (**Table 4**) is in agreement with such an interaction.

For the potentiometric titrations of the copper(II) complexes with **cb-te1pyp**<sup>2-</sup>, the solutions were prepared in an acidic medium (pH  $\sim$  2.5) and equilibrated for the time necessary to reach fully stabilized measurements thus allowing the determination of the corresponding stability constants. Due to the impossibility of determining the value for the first protonation constant of **cb-te1pyp**<sup>2-</sup>, only the ratio of the constants  $K_{\text{Cu-cb-te1pyp}}/K_{\text{Cb-te1pypH}}$  could be obtained ( $\log K_{\text{Cu-cb-te1pyp}} - \log K_{\text{Cb-te1pypH}} = 13.03(4)$ ) by this potentiometric approach. To further confirm our hypotheses and evaluate the value of the first protonation constant, a batch titration by UV-Vis. absorption spectrophotometry of **cb-te1pyp**<sup>2-</sup> by Cu(II) was carried out under acidic conditions and allowed the determination of the conditional formation constant of the corresponding cupric complex (*vide supra* for **te1pyp**<sup>2-</sup>, ESI, Figure S10). Only a monocupric monochelate with a conditional stability constant  $\log K^{\text{Cu-cb-te1pyp}} = 6.3(7)$  at pH 2.10 was evidenced. Assuming the value of first protonation constant to be about  $\log K_{\text{Cb-te1pypH}} = 13$ , a theoretical conditional constant  $\log K^{\text{Cu-cb-te1pyp}} = 5.8$  can be estimated in good agreement within experimental errors with the experimental value. Similarly to its [Cu(**te1pyp**)] analogue (*vide supra*), a protonation constant ( $\log K_{\text{Cu-te1pypH}} = 5.29(4)$ ) of the [Cu(**cb-te1pyp**)] complex was measured and most likely corresponds to the protonation of one oxygen atom

from the phosphonate moiety in agreement with solid-state data (**Figure 2**).

In addition to the potentiometric investigations, a UV-Vis. absorption characterization of the monocupric chelates as a function of pH was also performed (**Figure 7** and ESI, Figures S6 and S9). For **cb-te1pyp**<sup>2-</sup>, the prepared solution was set aside enough time to reach equilibrium prior to titration. The high stabilities of both copper(II) complexes even in highly acidic media were demonstrated by the presence of spectroscopic signatures such as intense  $\text{N} \rightarrow \text{Cu}^{2+}$  Charge Transfer (LMCT)<sup>51-53</sup> absorptions in the UV region and weaker  $\text{Cu}^{2+}$  d-d transitions in the visible spectral window (ESI, Figures S6 and S9). The statistical processing of the absorption and potentiometric data sets allowed the determination of the protonation equilibrium whose  $\text{pK}_a$  values ( $\log K_{\text{Cu-te1pypH}} = 5.8(2)$  for [Cu(**te1pyp**)] and  $\log K_{\text{Cu-cb-te1pypH}} = 5.4(7)$  for [Cu(**cb-te1pyp**)] were found to be in good agreement with those determined by pure potentiometry (Table 3). The spectral characteristics of the  $\text{Cu}^{2+}$  d-d transitions ( $\lambda_{\text{max}} = 542$  nm,  $\epsilon^{542} = 180$  M<sup>-1</sup> cm<sup>-1</sup>) with [Cu(**te1pyp**)] suggest a distorted square pyramidal geometry in agreement with the equal involvement of the four macrocyclic nitrogen atoms to  $\text{Cu}^{2+}$  binding and the apical binding of the *N*-pyridine unit ((**Figure 2** and ESI, Figures S6, S7 and S15).<sup>54,55</sup> On the other hand, it is noteworthy that these stereochemical properties are not markedly influenced by deprotonation of the phosphonate unit, emphasizing the absence of direct interaction of this unit with the metal center. These data are in excellent agreement with those obtained for the copper(II) complexes with the picolinate-derived analogue **te1pa**<sup>-</sup> ( $\lambda_{\text{max}} = 556$  nm,  $\epsilon^{542} = 197$  M<sup>-1</sup> cm<sup>-1</sup>) that displays the same coordination behavior with respect to Cu(II) with no

pH dependence on the *d-d* transitions.<sup>13</sup> Incorporation of the cross-bridge to the tetraazamacrocycle scaffold altered significantly the spectral characteristics of the Cu<sup>2+</sup> *d-d* transitions. The *d-d* transitions of [Cu(**cb-te1pyp**)] at pH ~ 2.5 are indeed characterized by two broad absorption bands in the visible ( $\lambda_{\text{max}} = 597 \text{ nm}$ ,  $\epsilon^{597} = 250 \text{ M}^{-1} \text{ cm}^{-1}$ ) and NIR ( $\lambda_{\text{max}} = 947 \text{ nm}$ ,  $\epsilon^{947} = 170 \text{ M}^{-1} \text{ cm}^{-1}$ ) spectral ranges thus demonstrating a significant change of the coordination geometry (Figure 2). Similarly to the picolinate analogue [Cu(**cb-te1pa**)], the *d-d* transitions of [Cu(**cb-te1pyp**)] are not sensitive to the acidity of the medium. Our observations thus match perfectly those obtained for [Cu(**cb-te1pa**)] ( $\lambda_{\text{max}} = 600 \text{ nm}$ ,  $\epsilon^{600} = 234 \text{ M}^{-1} \text{ cm}^{-1}$  and  $\lambda_{\text{max}} = 938 \text{ nm}$ ,  $\epsilon^{938} = 152 \text{ M}^{-1} \text{ cm}^{-1}$ ).<sup>14</sup> For the latter cupric complex, these spectral features were suggested to arise from a combination of the two geometries occurring in solution, a trigonal bipyramidal (*i.e.*, as observed in the solid state for [Cu(**cb-te1pyp**)], Figure 2) and a compressed octahedral (*i.e.* involving weak binding of a solvent molecule or hydroxide ion) geometries.<sup>12</sup> We therefore hypothesize the same properties in solution for the [Cu(**cb-te1pyp**)] complex.

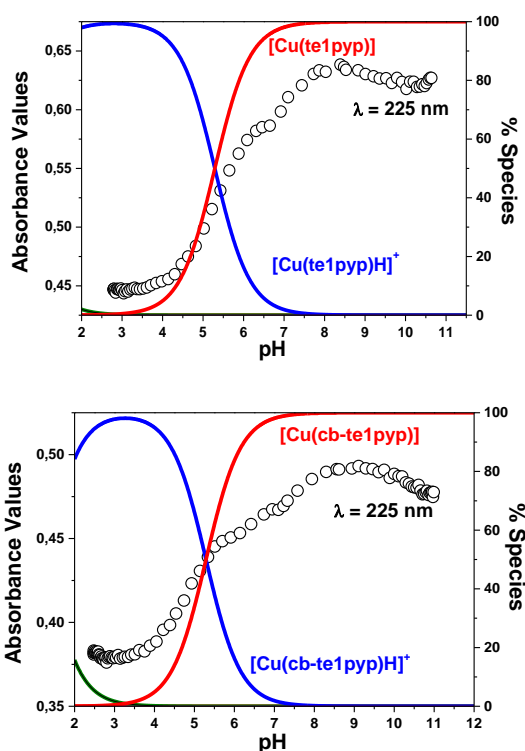


**Figure 7.** Distribution diagrams of the cupric complexes with **te1pyp**<sup>2-</sup> and **cb-te1pyp**<sup>2-</sup> in solution (from potentiometric data) as a function of pH, compared to the variation of the absorbance at 225 nm as a function of the pH.

To compare the coordination properties of H<sub>2</sub>**te1pyp** and H<sub>2</sub>**cb-te1pyp** with other copper(II) chelators, their pCu values (Table 4) were calculated at pH = 7.4.<sup>56,57</sup> These pCu values measure the equilibrium concentrations of free Cu<sup>2+</sup> ion and are defined as:  $\text{pCu} = -\log [\text{Cu}^{2+}]_{\text{free}}$  with  $[\text{L}]_{\text{tot}} = 10^{-5} \text{ M}$ ,  $[\text{Cu}^{2+}]_{\text{tot}} = 10^{-6} \text{ M}$ . This pCu value takes into account the characteristics of the ligands that are compared (acid-base properties of the free ligand and of the metal complexes,

stoichiometry of metal complexes, etc) and thus allows a direct comparison of their chelating affinity for a given cation. High pCu values will therefore be a signature of a strong binding affinity of the chelator toward Cu<sup>2+</sup>. For **te1pyp**<sup>2-</sup> and **cb-te1pyp**<sup>2-</sup>, the stability constants (Table 3) indicate high thermodynamic stabilities of the copper(II) complexes that are suitable for PET imaging techniques. Furthermore, the calculated pCu values (19.89 for H<sub>2</sub>**te1pyp** and 17.40 for H<sub>2</sub>**cb-te1pyp**) are comparable to the prototypical **cyclam** (pCu = 20.04) and its cross-bridged analogue **cb-cyclam** (pCu = 20.23). On the other hand, similar Cu(II) coordination properties have been evidenced in this report with the picolinate-derived chelators **Hte1pa** (pCu = 19.59) and **Hcb-te1pa** (pCu = 16.62).

**Kinetic Stability of the Copper(II) Complexes.** The kinetic inertness of such chelates can be estimated through acid-assisted dissociation in highly acidic media, to compare their properties to parent complexes. The dissociation was monitored by following the Cu-centered *d-d* absorption bands of the complexes under pseudo first-order conditions in aqueous solutions at 25 °C. [Cu(**te1pyp**)] and [Cu(**cb-te1pyp**)] exhibited half-lives of 35 min and 15.2 h respectively in 1 M HCl. In addition, [Cu(**cb-te1pyp**)] showed a half-life of 36 min in 5 M HCl at 25 °C (Table 5).

**Table 5.** Half-life ( $t_{1/2}$ ) values for copper(II) complexes of **te1pyp**, **cb-te1pyp** and their picolinate analogues in acidic conditions.

Ligands	<b>te1pyp</b>	<b>cb-te1pyp</b>	<b>te1pa</b> <sup>13</sup>	<b>cb-te1pa</b> <sup>14</sup>
Conditions	$t_{1/2}$			
1M HCl, 25°C	35 min	912 min	32 min	
5M HCl, 25°C		36 min		465 min

The kinetic inertness of [Cu(**te1pyp**)] parallels its picolinate analogue [Cu(**te1pa**)]. In accordance with previously described trends, the corresponding cross-bridged complex [Cu(**cb-te1pyp**)] presents a much higher inertness owing to the reinforced and preorganized cavity, but remains lower than its picolinate counterpart, evidencing again the effect of phosphonate moieties in this regard. However, these data provide a good indication towards the safe use *in vivo* for both complexes.

**<sup>64</sup>Cu-Radiolabeling and *in vitro* stability.** Radiolabeling was performed using similar conditions previously described for the picolinate analogues, *i.e.* pH 5-6 in sodium acetate buffer solutions, and incubation times of 30 minutes at 40 °C and 85 °C respectively for H<sub>2</sub>**te1pyp** and H<sub>2</sub>**cb-te1pyp**. Quantitative labeling was observed by C<sub>18</sub>-silica radio-TLC, and radio-HPLC experiments confirmed the purity of the samples (see ESI, Figure S17). To corroborate the kinetic inertness experiments, stability in human serum was also investigated for the least inert [<sup>64</sup>Cu(**te1pyp**)], with <sup>64</sup>Cu acetate and [<sup>64</sup>Cu(**te1pa**)] in buffer solutions as controls (Figure 8).

After incubation at 37 °C, no dissociation is observed for [<sup>64</sup>Cu(**te1pyp**)] after 15 or 40 hours, exemplified by the

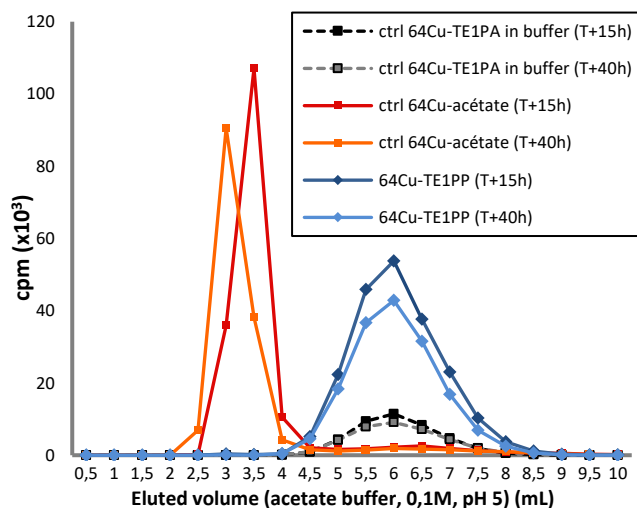


**Figure 8.** Radio-HPLC chromatograms of [ $^{64}\text{Cu}(\text{te1pyp})$ ] incubated in human serum for 15 and 40 hours.  $^{64}\text{Cu}$  acetate and a solution of [ $^{64}\text{Cu}(\text{te1pa})$ ] in acetate buffer were used as controls.

absence of a peak on radio-HPLC chromatograms at the retention time corresponding to protein-ligated  $^{64}\text{Cu}$  formed from free  $^{64}\text{Cu}$  acetate incubated in serum (3-3.5 mins). In addition, the complex is eluted with the same retention time as its [ $^{64}\text{Cu}(\text{te1pa})$ ] counterpart, furthermore evidencing its preservation. In order to confirm the absence of fixation to proteins and the intact nature of the chelate, a second control was realized by deproteinization of the samples and radio-TLC chromatography with  $^{64}\text{Cu}$ -acetate and  $^{64}\text{Cu}(\text{te1pyp})$  solution in buffer as controls. Again, the preserved complexes were unambiguously identified (see ESI, Figure S18).

***In vivo PET imaging and distribution.*** Owing to the excellent properties of both complexes *in vitro*, the *in vivo* behaviour of [ $^{64}\text{Cu}(\text{te1pyp})$ ] and [ $^{64}\text{Cu}(\text{cb-te1pyp})$ ] was investigated. 10 MBq of complexes were intravenously injected to Balb-C type mice, and PET-CT imaging was conducted at  $t = 2$  h post-injection (PI). Very interestingly, and as anticipated for these two phosphonated chelates, the body clearance is fast and mainly through renal elimination, as evidenced by the strong activity in kidneys and bladder (Figure 9).

However, the most striking feature is related to the very low activity (2% ID/g) detected in the liver for both chelates, which is much lower than what has been described for their carboxylated counterparts, with a SUV of  $10,2 \pm 2$  % reported at  $t = 2$  h PI for [ $^{64}\text{Cu}(\text{te1pa})$ ].<sup>15</sup> This positive effect can be attributed, as expected, to the difference in charge and lipophilicity brought by phosphonic moieties as compared to their carboxylic counterparts.

## CONCLUSIONS

We have recently reported the strong potential of Hte1pa and its bifunctional analogues as performant chelating ligands for targeted *in vivo*  $^{64}\text{Cu}$ -PET imaging. In this work, we have prepared the corresponding phosphonated equivalent of Hte1pa and its cross-bridge reinforced analogue Hcb-

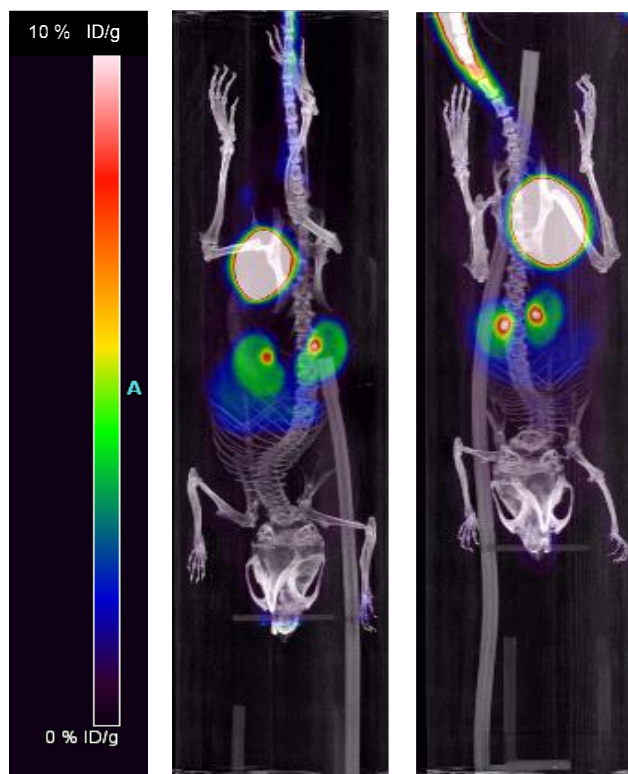


**Figure 9.** PET-CT imaging of Balb-C mice model injected with [ $^{64}\text{Cu}(\text{te1pyp})$ ] (left) and [ $^{64}\text{Cu}(\text{cb-te1pyp})$ ] (right) at  $t = 2$  h post-injection.

**te1pa**, and investigated their coordination properties towards copper(II) by solid-state, spectroscopic and potentiometric techniques. Both novel ligands demonstrated a high affinity for copper(II) and suitable kinetic inertness for *in vivo* use. Radiolabeling of the ligands was easily achieved in mild conditions, and full stability in human serum was evidenced. However, the biodistribution of the corresponding  $^{64}\text{Cu}$  complexes has been markedly improved compared to their picolinate analogues, with a fast renal elimination combined to very low hepatic fixation.  $\text{H}_2\text{te1pyp}$  and  $\text{H}_2\text{cb-te1pyp}$  corresponding bifunctional ligands will thus be considered in future work to enable their use in targeted PET imaging in oncology. Their reduced accumulation in the liver offers a great alternative when compared to their carboxylated congeners, to tune the biodistribution of corresponding radiotracers.

## EXPERIMENTAL SECTION

**Materials and methods.** Commercial grade chemicals and solvents were used without further purification. Where anhydrous solvents were used, they were degassed with  $\text{N}_2$  and passed through an MBraun MPSP-800 column, except in the case of anhydrous THF, which was dried over Na/benzophenone, vacuum distilled, degassed and stored over  $3\text{\AA}$  molecular sieves. Molecular sieves were activated by heated at  $200\text{ }^\circ\text{C}$  under dynamic vacuum for 18 hours. Where degassed solvents were used, they were degassed via freeze-pump-thaw (3-cycles) and stored over an atmosphere of argon. De-ionized water dispensed from a Millipore Milli-Q purification system was used in all cases. NMR

spectra were recorded with Bruker Avance 500 (500 MHz), Bruker Avance 400 (400 MHz), or Bruker AMX-3000 (300 MHz) spectrometers. All chemical shift ( $\delta$ ) values are given in parts per million and are referenced to the solvent. All coupling constants are quoted in Hz. All  $^{31}\text{P}$  and  $^{13}\text{C}$  spectra are proton decoupled unless otherwise stated, all  $^{13}\text{C}$  experiments were performed using the APT pulse sequence. In cases where solvent mixtures are used, the main solvent is used as the reference. Where an apparent multiplet (e.g. app. t.) is quoted,  $J_{\text{app}}$  is given. Accurate masses were determined to four decimal places; HR-MS analyses were performed at ICOA, Orléans, France. Elemental analysis were carried out by the Service Commun d'Analyses of the University of Strasbourg and were used to determine the HCl content of the synthesized ligands. (Boc) $_3$ cyclam, $^{32}$  cb-cyclam, $^{58}$  and diethyl (6-(chloromethyl)pyridin-2-yl)phosphonate $^{29}$  were synthesized as previously described.

**Synthesis of 1.** (Boc) $_3$ cyclam (1.269 g, 2.53 mmol, 1.0 eq.), diethyl (6-(chloromethyl)pyridin-2-yl)phosphonate (0.668 g, 2.534 mmol, 1.0 eq.),  $\text{K}_2\text{CO}_3$  (0.384 g, 2.78 mmol, 1.1 eq.) and NaI (0.416 g, 2.78 mmol, 1.1 eq.) were dissolved in anhydrous MeCN (40 mL) under an  $\text{N}_2$  atmosphere. The reaction was stirred at 40 °C for 48 hours. The reaction was filtered and the solvent removed *in vacuo*. The crude material was purified by column chromatography ( $\text{SiO}_2$ ; EtOAc/hex; 0:100→100: 0) to obtain **1** as an off-white foamy solid (1.061 g, 1.45 mmol, 58%).  $^1\text{H}$  NMR (300 MHz, 298 K,  $\text{CDCl}_3$ ) 7.72 – 7.57 (m, 2H, PyH), 7.39 (d,  $^3J_{\text{HH}} = 7.6$ , 1H, PyH), 4.08 (q,  $^3J_{\text{HH}} = 7.2$ , 4H,  $\text{PCH}_2\text{CH}_3$ ), 3.68 (s, 2H,  $\text{NCH}_2\text{Py}$ ), 3.44 – 3.01 (m, 12H,  $\text{NCH}_2$ ), 2.55 (br. s, 2H,  $\text{NCH}_2$ ), 2.35 (br. s, 2H,  $\text{NCH}_2$ ), 1.76 (br. s, 2H,  $\text{NCH}_2$ ), 1.57 (br. s, 2H,  $\text{NCH}_2$ ), 1.31 (d,  $^3J_{\text{HH}} = 5.6$ , 18H), 1.20 (t,  $^3J_{\text{HH}} = 7.1$ , 6H);  $^{13}\text{C}$  NMR (76 MHz, 298 K,  $\text{CDCl}_3$ ) 160.52 (d,  $^3J_{\text{PC}} = 23.7$ , Py), 155.40 (s,  $\text{NCO}_2^t\text{Bu}$ ), 150.93 (d,  $^1J_{\text{PC}} = 228.2$ , Py), 136.08 (d,  $^3J_{\text{PC}} = 11.2$ , Py), 126.27 (d,  $^2J_{\text{PC}} = 25.0$ , Py), 125.30 (s, Py), 79.30 ( $\text{NCH}_2\text{Py}$ ), 62.73 (d,  $^2J_{\text{PC}} = 6.1$ ,  $\text{PCH}_2\text{CH}_3$ ), 60.63 (s,  $\text{NCH}_2$ ), 51.90 (s,  $\text{NCH}_2$ ), 47.70 (s,  $\text{NCH}_2$ ), 47.44 (s,  $\text{NCH}_2$ ), 47.02 (s,  $\text{NCH}_2$ ), 46.79 (s,  $\text{NCH}_2$ ), 45.92 (s,  $\text{NCH}_2$ ), 28.33 (s,  $\text{POCH}_2\text{CH}_3$ ), 28.25 (s,  $^t\text{Bu}$ ), 16.22 (d,  $^2J_{\text{PC}} = 6.1$ ,  $\text{POCH}_2\text{CH}_3$ );  $^{31}\text{P}$  NMR (162 MHz, 298 K,  $\text{CDCl}_3$ ) 12.1 (s); ESI-HRMS  $m/z$  calcd. for  $[\text{C}_{35}\text{H}_{63}\text{N}_5\text{O}_9\text{P} + \text{H}]^+$  728.4358, found 728.4345.

**Synthesis of H<sub>2</sub>te1pyp.2HCl.** Boc $_3$ te1pyp ester (1.081 g, 1.45 mmol) was dissolved in 6 M  $\text{HCl}_{(\text{aq})}$  (20 mL) and heated at 110 °C for 48 hours. The reaction mixture was cooled and the solvent removed *in vacuo*. The crude material was dissolved in a minimum of  $\text{H}_2\text{O}$  (ca. 5 mL) and layered with acetone (ca. 100 mL) to obtain  $\text{H}_2\text{te1pyp.2HCl}$  as a white solid (570 mg, 1.29 mmol, 89%).  $^1\text{H}$  NMR (400 MHz, 298 K,  $\text{D}_2\text{O}$ ) 8.27 (m, 1H, Py), 8.02 (t,  $^3J_{\text{HH}} = 7.3$ , 1H, PyH), 7.80 (d,  $^3J_{\text{HH}} = 7.9$ , 1H, PyH), 4.11 (s, 2H,  $\text{NCH}_2\text{Py}$ ), 3.55 (t,  $^3J_{\text{HH}} = 6.5$ , 2H,  $\text{NCH}_2$ ), 3.47 – 3.28 (m, 8H,  $\text{NCH}_2$ ), 3.20 (t,  $^3J_{\text{HH}} = 7.1$ , 2H,  $\text{NCH}_2$ ), 3.04 (t,  $^3J_{\text{HH}} = 5.8$ , 2H,  $\text{NCH}_2$ ), 2.86 (t,  $^3J_{\text{HH}} = 6.0$ , 2H,  $\text{NCH}_2$ ), 2.27 – 2.19 (m, 2H,  $\text{NCH}_2\text{CH}_2$ ), 2.01 (q,  $^3J_{\text{HH}} = 6.6$ , 2H,  $\text{NCH}_2\text{CH}_2$ );  $^{13}\text{C}$  NMR (75 MHz, 298 K,  $\text{D}_2\text{O}$ ) 154.06 (d,  $^1J_{\text{PC}} = 185.2$ , Py), 152.84 (d,  $^3J_{\text{PC}} = 10.7$ , Py), 145.89 (d,  $^3J_{\text{PC}} = 9.3$ , Py), 128.96 (d,  $^2J_{\text{PC}} = 14.4$ , Py), 128.76 (s, Py), 57.38 ( $\text{NCH}_2\text{Py}$ ), 52.01 ( $\text{NCH}_2$ ), 49.13 ( $\text{NCH}_2$ ), 43.80 ( $\text{NCH}_2$ ), 43.35 ( $\text{NCH}_2$ ), 43.12 ( $\text{NCH}_2$ ), 42.92 ( $\text{NCH}_2$ ), 40.51 ( $\text{NCH}_2$ ), 39.72 ( $\text{NCH}_2$ ), 22.66 ( $\text{NCH}_2\text{CH}_2$ ), 20.91 ( $\text{NCH}_2\text{CH}_2$ );  $^{31}\text{P}$  NMR (162 MHz, 298 K,  $\text{D}_2\text{O}$ ) 2.6 (s); ESI-HRMS  $m/z$  calcd. for

$[\text{C}_{16}\text{H}_{10}\text{N}_5\text{O}_3\text{P} + \text{H}]^+$  372.2159, found 372.2159; UV/vis (Tris Buffer $_{(\text{aq})}$  0.1 M)  $\lambda_{\text{max}}$ ; 227 (3200), 285 (3400).

**Synthesis of 2.** Diethyl (6-(chloromethyl)pyridin-2-yl)phosphonate (243 mg, 0.884 mmol, 1.0 eq.) was dissolved in anhydrous MeCN (20 mL) and added dropwise over 20 hours to a solution of CB-cyclam (200 mg, 0.884 mmol, 1.0 eq.) in anhydrous MeCN (175 mL) under an  $\text{N}_2$  atmosphere. The reaction was stirred at ambient temperature for 36 hours, filtered and the solvent removed *in vacuo*. The crude material was purified by column chromatography ( $\text{SiO}_2$ ;  $\text{CH}_2\text{Cl}_2/\text{MeOH}$ ; 100:0→90:10) to obtain cbte1pyp ester.HCl as an off-white foamy solid (345 g, 0.74 mmol, 84%).  $^1\text{H}$  NMR (400 MHz, 298 K,  $\text{CDCl}_3$ ) 11.48 (s, 1H,  $\text{NHH}$ ), 8.86 (s, 1H,  $\text{NHH}$ ), 7.84 – 7.72 (m, 1H, PyH), 7.66 (t,  $^3J_{\text{HH}} = 7.0$ , 1H, PyH), 7.45 (d,  $^3J_{\text{HH}} = 7.8$ , 1H, PyH), 4.16 – 3.96 (m, 6H,  $\text{NCHHPy} + \text{POCH}_2\text{CH}_3$ ), 3.52 (d,  $^3J_{\text{HH}} = 12.6$ , 1H,  $\text{NCHHPy}$ ), 3.41 (s, 1H,  $\text{NCH}_2$ ), 3.15 – 2.35 (m, 20H,  $\text{NCH}_2$ ), 1.91 – 1.74 (m, 1H,  $\text{NCH}_2\text{CH}_2$ ), 1.58 (s, 1H,  $\text{NCH}_2\text{CH}_2$ ), 1.43 – 1.29 (m, 1H,  $\text{NCH}_2\text{CH}_2$ ), 1.22 (m, 6H,  $\text{POCH}_2\text{CH}_3$ ), 1.12 – 1.01 (m, 1H,  $\text{NCH}_2\text{CH}_2$ );  $^{13}\text{C}$  NMR (76 MHz, 298 K,  $\text{CDCl}_3$ ) 159.12 (d,  $^3J_{\text{PC}} = 21.7$ , Py), 150.70 (d,  $^1J_{\text{PC}} = 225.9$ , Py), 137.45 (d,  $^3J_{\text{PC}} = 12.0$ , Py), 127.59 (d,  $^4J_{\text{PC}} = 3.3$ , Py), 126.05 (d,  $^3J_{\text{PC}} = 23.4$ , Py), 63.10 – 62.50 (m,  $\text{POCH}_2\text{CH}_3 + \text{NCH}_2\text{Py}$ ), 57.57 (s,  $\text{NCH}_2$ ), 55.06 (s,  $\text{NCH}_2$ ), 54.86 (s,  $\text{NCH}_2$ ), 53.73 (s,  $\text{NCH}_2$ ), 52.99 (s,  $\text{NCH}_2$ ), 52.69 (s,  $\text{NCH}_2$ ), 51.62 (s,  $\text{NCH}_2$ ), 49.80 (s,  $\text{NCH}_2$ ), 46.75 (s,  $\text{NCH}_2$ ), 44.27 (s,  $\text{NCH}_2$ ), 26.65 (s,  $\text{NCH}_2$ ), 20.94 (s,  $\text{NCH}_2$ ), 16.02 (d,  $^4J_{\text{PC}} = 5.0$ ,  $\text{POCH}_2\text{CH}_3$ );  $^{31}\text{P}$  NMR (162 MHz, 298 K,  $\text{CDCl}_3$ ) 11.5 (s); ESI-HRMS  $m/z$  calcd. for  $[\text{C}_{22}\text{H}_{41}\text{N}_5\text{O}_3\text{P} + \text{H}]^+$  454.2942, found 454.29413.

**Synthesis of H<sub>2</sub>cb-te1pyp.2HCl.** CB-te1pyp ester (345 mg, 0.704 mmol) was dissolved in 6 M  $\text{HCl}_{(\text{aq})}$  (20 mL) and heated at 110 °C for 48 hours. The reaction mixture was cooled and the solvent removed *in vacuo*. The crude brown material was dissolved in a minimum of EtOH (ca. 5 mL), filtered and the solvent removed *in vacuo*. The resulting material was dissolved in MeOH (ca. 3 mL), precipitated with acetone (ca. 20 mL), filtered and the solvent removed *in vacuo*. The resulting solid was dissolved in MeOH (ca. 3 mL) and precipitated with THF (ca. 20 mL), filtered and washed with THF (3 × 5 mL) to give  $\text{H}_2\text{cb-te1pyp.2HCl}$  as a white solid (200 mg, 0.42 mmol, 60%).  $^1\text{H}$  NMR (300 MHz, 298 K,  $\text{D}_2\text{O}$ ) 7.92 – 7.83 (m, 1H, PyH), 7.76 (t,  $^3J_{\text{HH}} = 7.2$ , 1H, PyH), 7.48 (d,  $^3J_{\text{HH}} = 7.7$ , 1H, PyH), 4.84 (d,  $^2J_{\text{HH}} = 14.2$ , 1H,  $\text{NCHHAr}$ ), 3.99 (d,  $^2J_{\text{HH}} = 14.2$ , 1H,  $\text{NCHHAr}$ ), 3.81 (dt,  $^2J_{\text{HH}} = 13.9$ ,  $^3J_{\text{HH}} = 7.1$ , 1H,  $\text{NCH}_2$ ), 3.50 – 3.13 (m, 6H,  $\text{NCH}_2$ ), 3.17 – 2.78 (m, 7H,  $\text{NCH}_2$ ), 2.77 – 2.57 (m, 2H,  $\text{NCH}_2$ ), 2.57 – 2.16 (m, 6H,  $\text{NCH}_2 + \text{NCH}_2\text{CH}_2$ ), 1.51 (app. dd,  $J_{\text{app}} = 35.4$ ,  $J_{\text{app}} = 16.6$ , 2H,  $\text{NCH}_2\text{CH}_2$ );  $^{13}\text{C}$  NMR (76 MHz, 298 K,  $\text{D}_2\text{O}$ ) 158.36 (d,  $^1J_{\text{PC}} = 210.4$ , Py), 152.47 (d,  $^3J_{\text{PC}} = 19.9$ , Py), 140.09 (d,  $^3J_{\text{PC}} = 11.0$ , Py), 128.68 (d,  $^4J_{\text{PC}} = 2.6$ , Py), 128.00 (d,  $^2J_{\text{PC}} = 22.3$ , Py), 59.25 (s,  $\text{NCH}_2$ ), 58.66 (s,  $\text{NCH}_2$ ), 58.05 (s,  $\text{NCH}_2$ ), 56.90 (s,  $\text{NCH}_2$ ), 55.82 (s,  $\text{NCH}_2$ ), 55.23 (s,  $\text{NCH}_2$ ), 50.99 (s,  $\text{NCH}_2$ ), 50.87 (s,  $\text{NCH}_2$ ), 50.33 (s,  $\text{NCH}_2$ ), 47.83 (s,  $\text{NCH}_2$ ), 42.98 (s,  $\text{NCH}_2$ ), 19.84 (s,  $\text{NCH}_2$ ), 19.29 (s,  $\text{NCH}_2$ );  $^{31}\text{P}$  NMR (162 MHz, 298 K,  $\text{D}_2\text{O}$ ) 7.9 (s); ESI-HRMS  $m/z$  calcd. for  $[\text{C}_{18}\text{H}_{33}\text{N}_5\text{O}_3\text{P} + \text{H}]^+$  398.2316, found 398.2319; UV/vis (Tris Buffer $_{(\text{aq})}$  0.1 M)  $\lambda_{\text{max}}$ ; 227 (4400), 285 (4600).

**Synthesis of Zn and Cu complexes (General Procedure).** Ligand (50 mg, 1.0 eq.) was dissolved in  $\text{H}_2\text{O}$  (3 mL), basified with a standard soln. of NaOH in  $\text{H}_2\text{O}$  (20 mM) to pH = 6.8.  $\text{M}(\text{ClO}_4)_2 \cdot 6\text{H}_2\text{O}$  (1.0 eq.) was added and the pH

equilibrated to pH = 7 and heated to 80 degrees for two hours. The solution was basified to pH = 6.8 and heated to 80 °C for 18 hours, after which the solution was acidified to pH = 3.5-4.0. The solvent was removed *in vacuo* and the crude reaction mixture was purified by C<sub>18</sub> (H<sub>2</sub>O/MeOH 100:0→80:20).

**Synthesis of [Zn(te1pyp)].** The title compound was synthesized according to the general procedure and obtained as a white solid (32 mg, 59.7 μmol, 57%). <sup>1</sup>H NMR (400 MHz, 298 K, D<sub>2</sub>O) 7.98 (td, <sup>3</sup>J<sub>HH</sub> = 7.7, <sup>4</sup>J<sub>HH</sub> = 3.3, 1H, PyH), 7.78 (s, 1H, PyH), 7.43 (d, <sup>3</sup>J<sub>HH</sub> = 7.9, 1H, PyH), 4.44 (br. s, 1H, NCHHAr), 3.80 (d, <sup>2</sup>J<sub>HH</sub> = 18.0, 1H, NCHHAr), 3.30 – 2.38 (m, 16H, NCH<sub>2</sub>), 1.85 (s, 4H, NCH<sub>2</sub>CH<sub>2</sub>); <sup>13</sup>C NMR (76 MHz, 298 K, D<sub>2</sub>O) *two conformations*; 163.3\*, 155.2\*, 140.34 (s, Py), 126.07 (d, J<sub>PC</sub> = 10.0, Py), 122.78 (d, J<sub>PC</sub> = 80.32, Py), 62.25 (s, NCH<sub>2</sub>), 60.35 (s, NCH<sub>2</sub>), 60.04 (s, NCH<sub>2</sub>), 56.57 (s, NCH<sub>2</sub>), 53.32 (s, NCH<sub>2</sub>), 52.76 (s, NCH<sub>2</sub>), 52.26 (s, NCH<sub>2</sub>), 50.90 (s, NCH<sub>2</sub>), 50.73 (s, NCH<sub>2</sub>), 50.49 (s, NCH<sub>2</sub>), 48.08 (s, NCH<sub>2</sub>), 45.74 (s, NCH<sub>2</sub>), 45.56 (s, NCH<sub>2</sub>), 44.38 (s, NCH<sub>2</sub>), 28.75 (s, NCH<sub>2</sub>CH<sub>2</sub>), 26.72 (s, NCH<sub>2</sub>CH<sub>2</sub>), 26.30 (s, NCH<sub>2</sub>CH<sub>2</sub>), 22.98 (s, NCH<sub>2</sub>CH<sub>2</sub>); \*located by HMBC. <sup>31</sup>P NMR (162 MHz, 298 K, D<sub>2</sub>O) *two conformations*; 7.3 (s), 5.1 (s); ESI-HRMS *m/z* calcd. for [C<sub>16</sub>H<sub>29</sub>N<sub>5</sub>O<sub>3</sub>PZn – ClO<sub>4</sub>]<sup>+</sup> 434.1294, found 434.1291.

**Synthesis of [Zn(cb-te1pyp)].** The title compound was synthesized according to the general procedure and obtained as a white solid (33 mg, 58.7 μmol, 60%). <sup>1</sup>H NMR (400 MHz, 298 K, D<sub>2</sub>O) 8.16 – 7.96 (m, 2H, PyH), 7.47 (d, <sup>3</sup>J<sub>HH</sub> = 7.4, 1H), 4.63 (d, <sup>2</sup>J<sub>HH</sub> = 16.5, 1H, NCHHAr), 3.95 – 3.85 (m, 1H, NCH<sub>2</sub>), 3.75 (d, <sup>2</sup>J<sub>HH</sub> = 16.5, 1H, NCHHAr), 3.71 – 3.51 (m, 3H, NCH<sub>2</sub>), 3.35 – 3.25 (m, 1H, NCH<sub>2</sub>), 3.15 – 2.90 (m, 8H, NCH<sub>2</sub>), 2.87 – 2.64 (m, 7H, NCH<sub>2</sub>), 2.58 – 2.27 (m, 3H, NCH<sub>2</sub> + NCH<sub>2</sub>CH<sub>2</sub>), 1.66 – 1.57 (m, 2H, NCH<sub>2</sub>CH<sub>2</sub>); <sup>13</sup>C NMR (76 MHz, 298 K, D<sub>2</sub>O) 166.09 (d, <sup>1</sup>J<sub>PC</sub> = 177.6, Py), 158.94 (d, <sup>3</sup>J<sub>PC</sub> = 13.4, Py), 142.80 (d, <sup>3</sup>J<sub>PC</sub> = 9.1, Py), 130.50 (d, <sup>2</sup>J<sub>PC</sub> = 15.3, Py), 127.44 (s, Py), 62.27 (s, NCH<sub>2</sub>), 61.78 (s, NCH<sub>2</sub>), 61.65 (s, NCH<sub>2</sub>), 60.60 (s, NCH<sub>2</sub>), 60.28 (s, NCH<sub>2</sub>), 57.40 (s, NCH<sub>2</sub>), 54.87 (s, NCH<sub>2</sub>), 54.61 (s, NCH<sub>2</sub>), 50.11 (s, NCH<sub>2</sub>), 49.65 (d, J<sub>PC</sub> = 13.0, NCH<sub>2</sub>), 44.28 (d, J<sub>PC</sub> = 12.6, NCH<sub>2</sub>), 24.20 (s, NCH<sub>2</sub>), 23.09 (s, NCH<sub>2</sub>). <sup>31</sup>P NMR (162 MHz, 298 K, D<sub>2</sub>O) 5.0 (s); ESI-HRMS *m/z* calcd. for [C<sub>18</sub>H<sub>31</sub>N<sub>5</sub>O<sub>3</sub>PZn – ClO<sub>4</sub>]<sup>+</sup> 460.1450, found 460.1448.

**Synthesis of [Cu(te1pyp)].** The title compound was synthesized according to the general procedure and obtained as a purple solid (63 mg, 118.1 μmol, 88%). ESI-HRMS *m/z* calcd. for [C<sub>16</sub>H<sub>29</sub>N<sub>5</sub>O<sub>3</sub>PCu – ClO<sub>4</sub>]<sup>+</sup> 433.1299, found 433.1295; UV/vis (H<sub>2</sub>O) λ<sub>max</sub>; 215 (4000), 274 (4300), 604 (200).

**Synthesis of [Cu(cb-te1pyp)].** The title compound was synthesized according to the general procedure and obtained as a blue solid (21 mg, 37.5 μmol, 38%). ESI-HRMS *m/z* calcd. for [C<sub>18</sub>H<sub>31</sub>N<sub>5</sub>O<sub>3</sub>PCu – ClO<sub>4</sub>]<sup>+</sup> 459.1455 found 459.1453; UV/vis (H<sub>2</sub>O) λ<sub>max</sub>; 229 (3500), 286 (4000), 555 (200), 937 (135).

**Physico-chemical studies, starting materials and solvents.** Distilled water was purified by passing it through a mixed bed of ion-exchanger (Bioblock Scientific R3-83002, M3-83006) and activated carbon (Bioblock Scientific ORC-83005) and was de-oxygenated by CO<sub>2</sub>- and O<sub>2</sub>-free argon (Sigma Oxiclear cartridge) just before use. The stock solutions were prepared by weighing solids using an AG 245

METTLER TOLEDO analytical balance (accuracy 0.01 mg). The ionic strength was maintained at 0.1 M with sodium chloride (NaCl, CARLO-ERBA-SDS PHAR. EUR. 99-100.5%), and all measurements were carried out at 25.0(2) °C. The copper(II) stock solutions (~ 5 x 10<sup>-2</sup> M) were prepared by dissolving appropriate amounts of solid Cu(II) perchlorate (Cu(ClO<sub>4</sub>)<sub>2</sub>·6H<sub>2</sub>O, Fluka, purum p.a., 99.3%) in water. The Cu(II) content was determined by colorimetric titrations.<sup>59</sup>

*CAUTION! Perchlorate salts combined with organic ligands are potentially explosive and should be handled in small quantities and with adequate precautions.*<sup>60</sup>

**Potentiometric titrations.** The potentiometric titrations of the free ligands **te1pyp**<sup>2-</sup> (1.26 × 10<sup>-3</sup> M) and **cb-te1pyp**<sup>2-</sup> (1.62 × 10<sup>-3</sup> M) and their cupric complexes (1.02 ≤ [Cu(II)]<sub>tot</sub>/[ligand]<sub>tot</sub> < 1.29) were performed using an automatic titrator system 794 Basic Titrino (Metrohm) with a combined glass electrode (Metrohm 6.0234.500, Long Life) filled with 0.1 M NaCl in water and connected to a micro-computer (Tiamo light 1.2 program). The combined glass electrode was calibrated as a hydrogen concentration probe by titrating known amounts of hydrochloric acid (~1.72 x 10<sup>-1</sup> M from HCl, Sigma-Aldrich, puriss pa, >37 %) with CO<sub>2</sub>-free sodium hydroxide solution (~ 9.8 x 10<sup>-2</sup> to 1.23 x 10<sup>-1</sup> M from NaOH, BdH, AnalaR, 98%).<sup>61</sup> The HCl and NaOH solutions were freshly prepared just before use and titrated with sodium tetraborate decahydrate (B<sub>4</sub>Na<sub>2</sub>O<sub>7</sub>·10H<sub>2</sub>O, Fluka, puriss, p.a., > 99.5%) and potassium hydrogen phthalate (C<sub>8</sub>H<sub>5</sub>KO<sub>3</sub>, Fluka, puriss, p.a., > 99.5%), respectively, with methyl orange (RAL) and phenolphthalein (Pro-labo, purum) used as colorimetric indicators. The temperature of the titration cell was maintained at 25.0 ± 0.2 °C with the help of a Lauda E200 thermostat. The Glee program<sup>61</sup> was applied for the glass electrode calibration (standard electrode potential E<sub>0</sub>/mV and slope of the electrode/mV pH<sup>-1</sup>) and to check carbonate levels of the NaOH solutions used (< 5 %). The potentiometric data of **te1pyp**<sup>2-</sup> and **cb-te1pyp**<sup>2-</sup> and their cupric complexes (about 300 points collected over the pH range 2.5-11.5) were refined with the Hyperquad 2000<sup>62</sup> program which uses non-linear least-squares methods.<sup>63</sup> Potentiometric data points were weighted by a formula allowing greater pH errors in the region of an end-point than elsewhere. The weighting factor W<sub>i</sub> is defined as the reciprocal of the estimated variance of measurements: W<sub>i</sub> = 1/σ<sub>i</sub><sup>2</sup> = 1/[σ<sub>E</sub><sup>2</sup> + (δE/δV)<sup>2</sup>σ<sub>V</sub><sup>2</sup>] where σ<sub>E</sub><sup>2</sup> and σ<sub>V</sub><sup>2</sup> are the estimated variances of the potential and volume readings, respectively. The constants were refined by minimizing the error-square sum, U, of the potentials: 
$$U = \sum_i^N W_i (E_{\text{obs}i} - E_{\text{calc}i})^2$$
. At least three potentiometric titrations were treated as single sets, for each system. The quality of fit was judged by the values of the sample standard deviation, S, and the goodness of fit, χ<sup>2</sup>, (Pearson's test). At σ<sub>E</sub> = 0.1 mV (0.023 σ<sub>pH</sub>) and σ<sub>V</sub> = 0.005 mL, the values of S in different sets of titrations were between 0.6 and 1.6, and χ<sup>2</sup> was below 99. The scatter of residuals vs. pH was reasonably random, without any significant systematic trends, thus indicating a good fit of the experimental data. The stability and successive protonation constants were calculated from the cumulative constants determined with the program. The uncertainties in the log K values correspond to the added standard deviations in the cumulative constants.

**Spectrophotometric Titrations vs. pH.** An aliquot of 40 mL of solutions containing  $\text{H}_2\text{te1pyp}$  ( $8.80 \times 10^{-5}$  M),  $\text{H}_2\text{cb-te1pyp}$  ( $1.12 \times 10^{-4}$  M),  $[\text{Cu}(\text{te1pyp})]$  ( $[\text{H}_2\text{te1pyp}]_0 = 1.39 \times 10^{-4}$  M and  $[\text{Cu}]_0 = 1.78 \times 10^{-4}$  M) or  $[\text{Cu}(\text{cb-te1pyp})]$  ( $[\text{H}_2\text{cb-te1pyp}]_0 = 1.11 \times 10^{-4}$  M and  $[\text{Cu}]_0 = 1.14 \times 10^{-4}$  M) were introduced in a jacketed cell (Metrohm) maintained at 25.0(2) °C (Lauda E200). The free hydrogen ion concentration was measured with a combined glass electrode (Metrohm 6.0234.500, Long Life) and an automatic titrator system 794 Basic Titrino (Metrohm). The Ag/AgCl reference glass electrode was filled with NaCl (0.1 M, Carlo-Erba-SDS Phar. Eur. 99-100.5%) and was calibrated as a hydrogen concentration probe as described above. The initial pH was adjusted to  $\sim 2.5$ -3.8 with HCl (Sigma-Aldrich, puriss pa, >37%) and the titrations of the ligands ( $\text{te1pyp}^{2-}$ :  $3.80 < \text{pH} < 11.01$  and  $\text{cb-te1pyp}^{2-}$ :  $2.94 < \text{pH} < 10.85$ ) or the cupric complexes ( $[\text{Cu}(\text{te1pyp})]$ :  $2.79 < \text{pH} < 10.64$  and  $[\text{Cu}(\text{cb-te1pyp})]$ :  $2.48 < \text{pH} < 10.49$ ) were then carried out by automatic addition of known volumes of NaOH solutions (Bdh, AnalaR). After each addition (*i.e.*, volume of base/pH automatically adjusted according to the potentiometric signal drift of the solution with the Dynamic Potential Titration - DET - of the Tiamo program with a measuring point density of 3; duration between two additions of 210 s), an absorption spectrum was recorded using a Varian CARY 50 spectrophotometer fitted with Hellma optical fibres (Hellma, 041.002-UV) and an immersion probe made of quartz suprasil (Hellma, 661.500-QX) and interfaced (Cetrib) with the automatic titrator system 794 Basic Titrino.

**Spectrophotometric titrations of te1pyp and cb-te1pyp by Cu(II) at fixed pH.** Stock solutions of  $\text{H}_2\text{te1pyp}$  ( $1.01 \times 10^{-4}$  M) and  $\text{H}_2\text{cb-te1pyp}$  ( $6.48 \times 10^{-5}$  M) were prepared in acidic aqueous solutions. The spectrophotometric titrations of  $\text{te1pyp}^{2-}$  and  $\text{cb-te1pyp}^{2-}$  by Cu(II) were thus carried out on solutions at pH 1.53 ( $\text{te1pyp}^{2-}$ ) or at pH 2.10 ( $\text{cb-te1pyp}^{2-}$ ) with an ionic strength of 0.1 M (NaCl). For  $\text{te1pyp}^{2-}$  (*i.e.*, fast formation kinetics),  $\mu\text{volumes}$  of a concentrated solution of Cu(II) ( $1.64 \times 10^{-3}$  M) were added to 2.5 mL of the ligand solutions in a 1 cm path length optical cell (Hellma; the  $[\text{Cu}]_{\text{tot}}/[\text{te1pyp}]_{\text{tot}}$  ratio varied from 0 to 2.6). Special care was taken to ensure that complete equilibrium was attained. For  $\text{cb-te1pyp}^{2-}$ , the kinetics of cupric complex formation was too slow and required the equilibration of metal/ligand mixtures for one day (batch titration) to ensure that the samples reached equilibrium. The  $[\text{Cu}]_{\text{tot}}/[\text{cb-te1pyp}]_{\text{tot}}$  ratio varied from 0 to 1.4 and in a 1 cm path length optical cell (Hellma) was used. The corresponding UV-Vis spectra were then recorded from 220 nm to 1000 nm on a UV-Vis.-NIR Cary 5000 (Varian) spectrophotometer maintained at 25.0(2) °C by the flow of a Cary Varian Dual Cell Peltier accessory.

**Analysis and Processing of the Spectroscopic Data.** The spectrophotometric data were analysed with Specfit<sup>64-66</sup> program which adjusts the absorptivities and the stability constants of the species formed at equilibrium. Specfit uses factor analysis to reduce the absorbance matrix and to extract the eigenvalues prior to the multiwavelength fit of the reduced data set according to the Marquardt algorithm.<sup>67,68</sup>

**LC-MS Analysis of ligands and corresponding copper(II) complexes.** Copper complexes were analyzed with a Accela 600 liquid chromatography LC apparatus coupled

to a Thermo MSQ mass spectrometer (Thermo Fisher Scientific, San Jose, CA, USA). The sample (*ca.*  $3 \cdot 10^{-4}$  M) was dissolved in an acetonitrile/water mixture (20/80), 5  $\mu\text{L}$  of the stock solution was directly injected onto an Accucore C18 (2.7  $\mu\text{m}$  particle size,  $100 \times 2.1$  mm i.d.) fitted with hypersil pre-column (2.1 mm i.d., filter cartridge 0.2  $\mu\text{m}$ ) in an Accela 600 liquid chromatography apparatus. The chromatogram was recorded at a flow of 0.5 ml/min with a gradient from a buffer A (water with 0.1% formic acid) to a buffer B (MeCN with 0.1% formic acid). A 50:50 % split was applied dividing the flow in two parts, one for the mass detector and the other in the photodiode array. The LC was coupled to a Thermo MSQ mass spectrometer operated under a positive ionization mode with the following source settings: electro-spray source at 350 °C under  $\text{N}_2$  nebulisation at 5 bar. The cone voltage was applied to 75 V in positive mode with a scan time of 0.5 sec. Data acquisition was performed in full scan mode monitoring from 100 Dalton to 1000 Dalton. No fragmentation processes were observed under these experimental conditions. The photodiode array (PDA) was scanned from 200 to 600 nm. Wavelengths extractions were studied at 254 nm and 350 nm. Xcalibur software (Thermo version 2.1) was used for data registration

**Electron Paramagnetic Resonance Studies** Spectra were recorded at the 'Service Commun de RMN-RPE' at the Universite de Bretagne Occidentale (UBO) on an Bruker Elexsys 500 instrument, in a 0.5 mm capillary within a quartz tube, at 9.34 GHz (band X) using a complexes concentration of *ca.* 1.0 mM. EPR data simulations were performed using Easyspin<sup>69</sup> and Simultispin.<sup>70</sup>

**UV/vis and Kinetic Inertness Studies** UV-Vis and NIR spectra were recorded at 20°C on a Agilent Cary 5000 UV-Vis-NIR apparatus in 700 microliter cuvettes with 1 cm optical path, and baseline correction was applied. Acid-assisted dissociation experiments were carried out with a complex concentration of  $5 \times 10^{-3}$  M, in 700 microliter cuvettes on a JASCO V-760 spectrometer equipped with PAC-743R Peltier temperature control device.

**<sup>64</sup>Cu-Radiolabeling.** Copper-64 dichloride in 0.1M hydrochloric acid was kindly provided by ARRONAX cyclotron (Saint-Herblain, France). Radionuclidic purity was determined by gamma spectroscopy using a DSPEC-JR-2.0 type 98-24B HPGE detector (AMETEK) and chemical purity was controlled by ICP-OES with an iCAP 6500 DUO (Thermo Fisher Scientific). Radio-HPLC measurements were carried out on an Eckert&Ziegler HPLC Module, Modular-Lab software, Knauer pumps K120, Knauer HPLC Degasser, Knauer smartline UV 2520 ( $\lambda = 211$  nm), Eckert&Ziegler detector shielding module and ACE C18 column (3  $\mu$ ,  $150 \times 3$  mm).

Stock solutions of te1pyp and cb-te1pyp were made by dissolving 5mg of ligand (as the 2-HCl salts) in 1 milliliter of 1M sodium acetate. Radiolabeling was performed in triplicate with three distinct <sup>64</sup>Cu batches, from <sup>64</sup>CuCl<sub>2</sub> solutions in 0.1M HCl with a ligand/metal ratio between 65:1 and 80:1 (1MBq/ $\mu\text{g}$  of ligand). Incubation was set for 30 mins at 40°C for te1pyp and at 85°C for cb-te1pyp. Quantitative labeling was confirmed by radio-TLC that was carried out by deposition of 1  $\mu\text{L}$  of the crude mixture on C18-grafted silica plates, eluted with a 1:1 mixture of 20% ammonium chloride and methanol. Additional radio-HPLC controls were conducted on C18 ACE silica, through elution with a TFA /

Acetonitrile gradient ( $[^{64}\text{Cu}(\text{te1pyp})]$  and **cb-te1pyp** were detected at  $t = 5.42$  and  $5.40$  mins respectively, with no detection of free  $^{64}\text{Cu}$  at earlier retention times

**In vitro serum stability.** Human serum was supplied by Nantes university hospital biology platform. Samples were prepared through addition of  $70\mu\text{L}$  of  $[^{64}\text{Cu}(\text{te1pyp})]$ ,  $[^{64}\text{Cu}(\text{te1pa})]$  and  $^{64}\text{Cu}$  acetate to  $930\mu\text{L}$  of human serum (ca.  $3\text{MBq/mL}$ ) and incubated at  $37^\circ\text{C}$ . Samples were controlled after 15 and 40 hours by Radio-HPLC (PD10 column) with  $0.1\text{M}$  sodium acetate ( $\text{pH} = 5$ ) as eluant (Figure X).

After deproteinization of the samples with saturated ammonium sulfate, Radio-TLC-chromatography of the supernatant was conducted (solid phase : silica for te1pa group; C18-grafted silica for te1pyp group; eluant :  $20\%$  ammonium chloride / methanol 1:1) and revealed on a Cyclone Plus phosphor imager (Perkin Elmer))

**In vivo imaging.** Animal experiments were carried out in compliance with French regulation and approved by Ethics Committee for animal experimentation-Région Pays de la Loire (approval number: B-44-278) as protocol n° 00143.01. Mature (14–17 weeks old) female BALB/c wild were purchased from Janvier (Le Genest St Isle, France). Mice were housed under standard conditions (standard diet and water ad libitum) and maintained in post-entry quarantine for 15 days before experiments. Mice were isoflurane anesthetized 10 min before they were imaged, after a whole body scan, over 2 hours using a dynamic process with a Siemens microPET gamma camera.<sup>71,72</sup> Fusion computed images were obtained using Inveon Research Workplace (Siemens Healthcare)<sup>73</sup> software. Mice ( $n = 2$  per group; body weight  $20 \pm 2$  g) were injected via the tail vein with  $9.5 \pm 0.5$  MBq in  $100\mu\text{L}$  of  $[^{64}\text{Cu}(\text{te1pyp})]$  ( $40 \pm 5\mu\text{g}$ ) or  $[^{64}\text{Cu}(\text{cb-te1pyp})]$  ( $40 \pm 5\mu\text{g}$ ). The dose was diluted in  $0.1\text{M}$  sodium acetate and the syringes were weighted prior and following the injection.

## ASSOCIATED CONTENT

The Supporting Information contains  $^1\text{H}$ ,  $^{13}\text{C}$ , and  $^{31}\text{P}$  NMR, ESI-HRMS, HPLC-MS, UV-Vis and EPR spectra for ligands and corresponding complexes; figures for physico-chemical experiments; Figures of kinetic inertness studies; Radio HPLC and radio-TLC chromatograms.

## AUTHOR INFORMATION

### Corresponding Authors

\*Dr. Thibault Troadec, [thibault.troadec@univ-brest.fr](mailto:thibault.troadec@univ-brest.fr) ;

\*Pr. Raphaël Tripier, [raphael.tripier@univ-brest.fr](mailto:raphael.tripier@univ-brest.fr)

### ORCID

Richard C. Knighton : [0000-0002-0336-3718](https://orcid.org/0000-0002-0336-3718)

Thibault Troadec : [0000-0002-8005-4302](https://orcid.org/0000-0002-8005-4302)

Valérie Mazan : [0000-0001-9230-4404](https://orcid.org/0000-0001-9230-4404)

Séverine Marionneau-Lambot : [0000-0002-5041-8531](https://orcid.org/0000-0002-5041-8531)

Thomas Le Bihan : [0000-0002-6792-457X](https://orcid.org/0000-0002-6792-457X)

Nathalie Saffon-Merceron : [0000-0002-0301-4163](https://orcid.org/0000-0002-0301-4163)

Nathalie Le Bris : [0000-0002-6936-3876](https://orcid.org/0000-0002-6936-3876)

Michel Chérel : [0000-0001-6347-6848](https://orcid.org/0000-0001-6347-6848)

Alain Faivre-Chauvet : [0000-0003-3849-0087](https://orcid.org/0000-0003-3849-0087)

Mourad Elhabiri : [0000-0001-6371-7533](https://orcid.org/0000-0001-6371-7533)

Loïc J. Charbonnière : [0000-0003-0328-9842](https://orcid.org/0000-0003-0328-9842)

Raphaël Tripier : [0000-0001-9364-788X](https://orcid.org/0000-0001-9364-788X)

## Author Contributions

The manuscript was written through contributions of all authors. All authors have given approval to the final version of the manuscript.

## Notes

The authors declare no competing financial interest

## Acknowledgements

T.T., R.T., R.C.K, T.L.B. and N.L.B. are grateful to the Centre National de la Recherche Scientifique (CNRS) and the Université de Bretagne Occidentale (CEMCA UMR 6521) for financial support.

T.T. and R.C.K. acknowledge Région Bretagne (SAD Hypo-Trac) for funding, the RSC Research Fund (Grant no. RF19-0248) for the purchase of equipment, and N. Kervarec from the "Service commun de RMN-RPE" (Université de Bretagne Occidentale) for EPR measurements.

M.E., V.M. and L.J.C. are grateful to the Centre National de la Recherche Scientifique (CNRS) and the University of Strasbourg (LIMA UMR 7042 and IPHC UMR 7178) for financial support. M.E. and V.M. gratefully thank Matthieu Chessé for his help in measuring the LC-MS-ESI data

M.C. and A. F-C. thank the French National Agency for Research, call "Investissements d'Avenir" IRON LabEx n° ANR-11-LABX-0018-01, IGO LabEx n° ANR-11-LABX-0016-01, Siric ILIAD, DHU Oncogreff, ArronaxPlus Equipex n° ANR-11-EQPX-0004 and NEXt n° ANR-16-IDEX-0007 for financial support, and the Radioactivity Technical Platform and CIMA imaging platform.

## REFERENCES

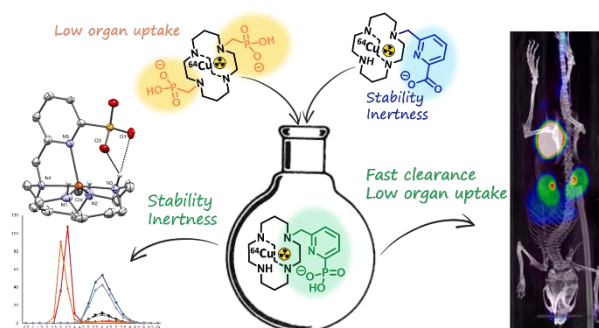
- (1) Heiden, M. G. V.; Cantley, L. C.; Thompson, C. B. Understanding the Warburg Effect: The Metabolic Requirements of Cell Proliferation. *Science* **2009**, *324* (5930), 1029–1033.
- (2) Belhocine, T.; Spaepen, K.; Dusart, M.; Castaigne, C.; Muylle, K.; Bourgeois, P.; Bourgeois, D.; Dierickx, L.; Flamen, P.  $^{18}\text{F}$ FDG PET in Oncology: The Best and the Worst (Review). *International Journal of Oncology* **2006**, *28* (5), 1249–1261.
- (3) Wadas, T. J.; Wong, E. H.; Anderson, G. R. W. and C. J. Copper Chelation Chemistry and Its Role in Copper Radiopharmaceuticals. *Current Pharmaceutical Design* **2007**, *13* (1), 3–16.
- (4) Cai, Z.; Anderson, C. J. Chelators for Copper Radionuclides in Positron Emission Tomography Radiopharmaceuticals. *Journal of Labelled Compounds and Radiopharmaceuticals* **2014**, *57* (4), 224–230.
- (5) Anderson, C. J.; Ferdani, R. Copper-64 Radiopharmaceuticals for PET Imaging of Cancer: Advances in Preclinical and Clinical Research. *Cancer Biotherapy and Radiopharmaceuticals* **2009**, *24* (4), 379–393.
- (6) Boswell, C. A.; Sun, X.; Niu, W.; Weisman, G. R.; Wong, E. H.; Rheingold, A. L.; Anderson, C. J. Comparative in Vivo Stability of Copper-64-Labeled Cross-Bridged and

- Conventional Tetraazamacrocyclic Complexes. *J. Med. Chem.* **2004**, *47* (6), 1465–1474.
- (7) Delgado, R.; Félix, V.; Lima, L. M. P.; Price, D. W. Metal Complexes of Cyclen and Cyclam Derivatives Useful for Medical Applications: A Discussion Based on Thermodynamic Stability Constants and Structural Data. *Dalton Trans.* **2007**, No. 26, 2734–2745.
  - (8) Bass, L. A.; Wang, M.; Welch, M. J.; Anderson, C. J. In Vivo Transchelation of Copper-64 from TETA-Octreotide to Superoxide Dismutase in Rat Liver. *Bioconjugate Chem.* **2000**, *11* (4), 527–532.
  - (9) Pandya, D. N.; Kim, J. Y.; Park, J. C.; Lee, H.; Phapale, P. B.; Kwak, W.; Choi, T. H.; Cheon, G. J.; Yoon, Y.-R.; Yoo, J. Revival of TE2A; a Better Chelate for Cu(II) Ions than TETA? *Chem. Commun.* **2010**, *46* (20), 3517–3519.
  - (10) Bhatt, N.; Soni, N.; Ha, Y. S.; Lee, W.; Pandya, D. N.; Sarkar, S.; Kim, J. Y.; Lee, H.; Kim, S. H.; An, G. I.; et al. Phosphonate Pendant Armed Propylene Cross-Bridged Cyclam: Synthesis and Evaluation as a Chelator for Cu-64. *ACS Med. Chem. Lett.* **2015**, *6* (11), 1162–1166.
  - (11) Wadas, T. J.; Anderson, C. J. Radiolabeling of TETA- and CB-TE2A-Conjugated Peptides with Copper-64. *Nature Protocols* **2006**, *1* (6), 3062–3068.
  - (12) Boswell, C. A.; McQuade, P.; Weisman, G. R.; Wong, E. H.; Anderson, C. J. Optimization of Labeling and Metabolite Analysis of Copper-64-Labeled Azamacrocyclic Chelators by Radio-LC-MS. *Nuclear Medicine and Biology* **2005**, *32* (1), 29–38.
  - (13) Lima, L. M. P.; Esteban-Gómez, D.; Delgado, R.; Platas-Iglesias, C.; Tripier, R. Monopicolinate Cyclen and Cyclam Derivatives for Stable Copper(II) Complexation. *Inorg. Chem.* **2012**, *51* (12), 6916–6927.
  - (14) Lima, L. M. P.; Halime, Z.; Marion, R.; Camus, N.; Delgado, R.; Platas-Iglesias, C.; Tripier, R. Monopicolinate Cross-Bridged Cyclam Combining Very Fast Complexation with Very High Stability and Inertness of Its Copper(II) Complex. *Inorg. Chem.* **2014**, *53* (10), 5269–5279.
  - (15) Frindel, M.; Camus, N.; Rauscher, A.; Bourgeois, M.; Alliot, C.; Barré, L.; Gestin, J.-F.; Tripier, R.; Faivre-Chauvet, A. Radiolabeling of HTE1PA: A New Monopicolinate Cyclam Derivative for Cu-64 Phenotypic Imaging. In Vitro and in Vivo Stability Studies in Mice. *Nucl. Med. Biol.* **2014**, *41*, e49–e57.
  - (16) Halime, Z.; Frindel, M.; Camus, N.; Orain, P.-Y.; Lacombe, M.; Chérel, M.; Gestin, J.-F.; Faivre-Chauvet, A.; Tripier, R. New Synthesis of Phenyl-Isothiocyanate C-Functionalised Cyclams. Bioconjugation and <sup>64</sup>Cu Phenotypic PET Imaging Studies of Multiple Myeloma with the Te2a Derivative. *Org. Biomol. Chem.* **2015**, *13* (46), 11302–11314.
  - (17) Frindel, M.; Sač, P. L.; Beyler, M.; Navarro, A.-S.; Saï-Maurel, C.; Alliot, C.; Chérel, M.; Gestin, J.-F.; Faivre-Chauvet, A.; Tripier, R. Cyclam Te1pa for <sup>64</sup>Cu PET Imaging. Bioconjugation to Antibody, Radiolabeling and Pre-clinical Application in Xenografted Colorectal Cancer. *RSC Adv.* **2017**, *7* (15), 9272–9283.
  - (18) Le Bihan, T.; Navarro, A.-S.; Bris, N. L.; Sač, P. L.; Gouard, S.; Haddad, F.; Gestin, J.-F.; Chérel, M.; Faivre-Chauvet, A.; Tripier, R. Synthesis of C-Functionalized TE1PA and Comparison with Its Analogues. An Example of Bioconjugation on 9E7.4 MAb for Multiple Myeloma <sup>64</sup>Cu-PET Imaging. *Org. Biomol. Chem.* **2018**, *16* (23), 4261–4271.
  - (19) Ševčík, R.; Vaněk, J.; Michalicová, R.; Lubal, P.; Hermann, P.; Santos, I. C.; Santos, I.; Campello, M. P. C. Formation and Decomplexation Kinetics of Copper(II) Complexes with Cyclen Derivatives Having Mixed Carboxylate and Phosphonate Pendant Arms. *Dalton Trans.* **2016**, *45* (32), 12723–12733.
  - (20) Kotek, J.; Lubal, P.; Hermann, P.; Císařová, I.; Lukeš, I.; Godula, T.; Svobodová, I.; Táborský, P.; Havel, J. High Thermodynamic Stability and Extraordinary Kinetic Inertness of Copper(II) Complexes with 1,4,8,11-Tetraazacyclotetradecane-1,8-Bis(Methylphosphonic Acid): Example of a Rare Isomerism between Kinetically Inert Penta- and Hexacoordinated Copper(II) Complexes. *Chemistry – A European Journal* **2003**, *9* (1), 233–248.
  - (21) Svobodová, I.; Havlíčková, J.; Plutnar, J.; Lubal, P.; Kotek, J.; Hermann, P. Metal Complexes of 4,11-Dimethyl-1,4,8,11-Tetraazacyclotetradecane-1,8-Bis(Methylphosphonic Acid) – Thermodynamic and Formation/Decomplexation Kinetic Studies. *European Journal of Inorganic Chemistry* **2009**, *2009* (24), 3577–3592.
  - (22) Stigers, D. J.; Ferdani, R.; Weisman, G. R.; Wong, E. H.; Anderson, C. J.; Golen, J. A.; Moore, C.; Rheingold, A. L. A New Phosphonate Pendant-Armed Cross-Bridged Tetraamine Chelator Accelerates Copper(II) Binding for Radiopharmaceutical Applications. *Dalton Trans.* **2010**, *39* (7), 1699–1701.
  - (23) Dale, A. V.; Pandya, D. N.; Kim, J. Y.; Lee, H.; Ha, Y. S.; Bhatt, N.; Kim, J.; Seo, J. J.; Lee, W.; Kim, S. H.; et al. Non-Cross-Bridged Tetraazamacrocyclic Chelator for Stable <sup>64</sup>Cu-Based Radiopharmaceuticals. *ACS Med. Chem. Lett.* **2013**, *4* (10), 927–931.
  - (24) Bass, L. A.; Wang, M.; Welch, M. J.; Anderson, C. J. In Vivo Transchelation of Copper-64 from TETA-Octreotide to Superoxide Dismutase in Rat Liver. *Bioconjugate Chem.* **2000**, *11* (4), 527–532.
  - (25) Ferdani, R.; Stigers, D. J.; Fiamengo, A. L.; Wei, L.; Li, B. T. Y.; Golen, J. A.; Rheingold, A. L.; Weisman, G. R.; Wong, E. H.; Anderson, C. J. Synthesis, Cu(II) Complexation, <sup>64</sup>Cu-Labeling and Biological Evaluation of Cross-Bridged Cyclam Chelators with Phosphonate Pendant Arms. *Dalton Trans.* **2012**, *41* (7), 1938–1950.
  - (26) Dale, A. V.; An, G. I.; Pandya, D. N.; Ha, Y. S.; Bhatt, N.; Soni, N.; Lee, H.; Ahn, H.; Sarkar, S.; Lee, W.; et al. Synthesis and Evaluation of New Generation Cross-Bridged Bifunctional Chelator for <sup>64</sup>Cu Radiotracers. *Inorg. Chem.* **2015**, *54* (17), 8177–8186.
  - (27) Sun, X.; Wuest, M.; Weisman, G. R.; Wong, E. H.; Reed, D. P.; Boswell, C. A.; Motekaitis, R.; Martell, A. E.; Welch, M. J.; Anderson, C. J. Radiolabeling and In Vivo Behavior of Copper-64-Labeled Cross-Bridged Cyclam Ligands. *J. Med. Chem.* **2002**, *45* (2), 469–477.
  - (28) Sun, X.; Wuest, M.; Kovacs, Z.; Sherry, D. A.; Motekaitis, R.; Wang, Z.; Martell, A. E.; Welch, M. J.; Anderson, C. J. In Vivo Behavior of Copper-64-Labeled Methanephosphonate Tetraaza Macrocyclic Ligands. *J. Biol. Inorg. Chem.* **2003**, *8* (1), 217–225.
  - (29) Salaam, J.; Tabti, L.; Bahamyrou, S.; Lecointre, A.; Hernandez Alba, O.; Jeannin, O.; Camerel, F.; Cianfèrani, S.; Bentouhami, E.; Nonat, A. M.; et al. Formation of Mono- and Polynuclear Luminescent Lanthanide Complexes Based on the Coordination of Preorganized Phosphonated Pyridines. *Inorg. Chem.* **2018**, *57* (10), 6095–6106.
  - (30) Nonat, A.; Bahamyrou, S.; Lecointre, A.; Przybilla, F.; Mély, Y.; Platas-Iglesias, C.; Camerel, F.; Jeannin, O.; Charbonnière, L. J. Molecular Upconversion in Water in Heteropolynuclear Supramolecular Tb/Yb Assemblies. *J. Am. Chem. Soc.* **2019**, *141* (4), 1568–1576.
  - (31) Knighton, R. C.; Soro, L. K.; Trodec, T.; Mazan, V.; Nonat, A. M.; Elhabiri, M.; Saffon-Merceron, N.; Djenad, S.; Tripier, R.; Charbonnière, L. J. Formation of Heteropol-

- ynuclear Lanthanide Complexes Using Macrocyclic Phosphonated Cyclam-Based Ligands. *Inorg. Chem.* **2020**, *59* (14), 10311–10327.
- (32) Herrero, C.; Quaranta, A.; Ghachtouli, S. E.; Vauzeilles, B.; Leibl, W.; Aukauloo, A. Carbon Dioxide Reduction via Light Activation of a Ruthenium–Ni(Cyclam) Complex. *Phys. Chem. Chem. Phys.* **2014**, *16* (24), 12067–12072.
- (33) Addison, A. W.; Rao, T. N.; Reedijk, J.; Rijn, J. van; Verschoor, G. C. Synthesis, Structure, and Spectroscopic Properties of Copper(II) Compounds Containing Nitrogen–Sulphur Donor Ligands; the Crystal and Molecular Structure of Aqua[1,7-Bis(N-Methylbenzimidazol-2'-Yl)-2,6-Dithiaheptane]Copper(II) Perchlorate. *J. Chem. Soc., Dalton Trans.* **1984**, No. 7, 1349–1356.
- (34) Lever, A. B. P. *Inorganic Electronic Spectroscopy*, 2nd Ed.; Elsevier, New York, 1984; pp 554–572.
- (35) Hathaway, B. J. Copper. *Coordination Chemistry Reviews* **1983**, *52*, 87–169.
- (36) Hathaway, B. J.; Tomlinson, A. A. G. Copper(II) Ammonia Complexes. *Coordination Chemistry Reviews* **1970**, *5* (1), 1–43.
- (37) Hathaway, B. J.; Billing, D. E. The Electronic Properties and Stereochemistry of Mono-Nuclear Complexes of the Copper(II) Ion. *Coordination Chemistry Reviews* **1970**, *5* (2), 143–207.
- (38) Bertini, I.; Gatteschi, D.; Scozzafava, A. Jahn-Teller Distortions of Tris(Ethylenediamine)Copper(II) Complexes. *Inorg. Chem.* **1977**, *16* (8), 1973–1976.
- (39) Halcrow, M. A. Interpreting and Controlling the Structures of Six-Coordinate Copper(II) Centres – When Is a Compression Really a Compression? *Dalton Trans.* **2003**, No. 23, 4375–4384.
- (40) Garribba, E.; Micera, G. The Determination of the Geometry of Cu(II) Complexes: An EPR Spectroscopy Experiment. *J. Chem. Educ.* **2006**, *83* (8), 1229.
- (41) Hancock, R. D.; Motekaitis, R. J.; Mashishi, J.; Cukrowski, I.; Reibenspies, J. H.; Martell, A. E. The Unusual Protonation Constants of Cyclam. A Potentiometric, Crystallographic and Molecular Mechanics Study. *J. Chem. Soc., Perkin Trans. 2* **1996**, No. 9, 1925–1929.
- (42) Micheloni, M.; Sabatini, A.; Paoletti, P. Solution Chemistry of Macrocycles. Part 1. Basicity Constants of 1,4,8,11-Tetra-Azacyclotetradecane, 1,4,8,12-Tetra-Azacyclopentadecane, and 1,4,8,11-Tetramethyl-1,4,8,11-Tetra-Azacyclopentadecane. *J. Chem. Soc., Perkin Trans. 2* **1978**, No. 8, 828–830.
- (43) Esteves, C. V.; Lamosa, P.; Delgado, R.; Costa, J.; Désogère, P.; Rousselin, Y.; Goze, C.; Denat, F. Remarkable Inertness of Copper(II) Chelates of Cyclen-Based Macrobicycles with Two Trans-N-Acetate Arms. *Inorg. Chem.* **2013**, *52* (9), 5138–5153.
- (44) Weisman, G. R.; Rogers, M. E.; Wong, E. H.; Jasinski, J. P.; Paight, E. S. Cross-Bridged Cyclam. Protonation and Lithium Cation (Li<sup>+</sup>) Complexation in a Diamond-Lattice Cleft. *J. Am. Chem. Soc.* **1990**, *112* (23), 8604–8605.
- (45) Bencini, A.; Bianchi, A.; Bazzicalupi, C.; Ciampolini, M.; Fusi, V.; Micheloni, M.; Nardi, N.; Paoli, P.; Valtancoli, B. Proton Inclusion Properties of a New Azamacrocycle. Synthesis, Characterization and Crystal Structure of [H3L][Cl]3·2H2O (L = 4,10-Dimethyl-1,4,7,10-Tetraazabicyclo [5.5.2] Tetradecane). *Supramolecular Chemistry* **1994**, *3* (2), 141–146.
- (46) Hubin, T. J.; McCormick, J. M.; Collinson, S. R.; Buchalova, M.; Perkins, C. M.; Alcock, N. W.; Kahol, P. K.; Raghunathan, A.; Busch, D. H. New Iron(II) and Manganese(II) Complexes of Two Ultra-Rigid, Cross-Bridged Tetraazamacrocycles for Catalysis and Biomimicry. *Journal of the American Chemical Society* **2000**, *122* (11), 2512–2522.
- (47) Bernier, N.; Costa, J.; Delgado, R.; Félix, V.; Royal, G.; Tripier, R. Trans-Methylpyridine Cyclen versus Cross-Bridged Trans-Methylpyridine Cyclen. Synthesis, Acid–Base and Metal Complexation Studies (Metal = Co<sup>2+</sup>, Cu<sup>2+</sup>, and Zn<sup>2+</sup>). *Dalton Trans.* **2011**, *40* (17), 4514–4526.
- (48) Gillet, R.; Roux, A.; Brandel, J.; Huclier-Markai, S.; Camerel, F.; Jeannin, O.; Nonat, A. M.; Charbonnière, L. J. A Bispidol Chelator with a Phosphonate Pendant Arm: Synthesis, Cu(II) Complexation, and <sup>64</sup>Cu Labeling. *Inorg. Chem.* **2017**, *56* (19), 11738–11752.
- (49) Charpentier, C.; Salaam, J.; Nonat, A.; Carniato, F.; Jeannin, O.; Brandariz, I.; Esteban-Gomez, D.; Platas-Iglesias, C.; Charbonnière, L. J.; Botta, M. PH-Dependent Hydration Change in a Gd-Based MRI Contrast Agent with a Phosphonated Ligand. *Chemistry – A European Journal* **2020**, *26* (24), 5407–5418.
- (50) Ringbom, A. *Les Complexes En Chimie Analytique*; Ed. Dunod, France, 1967; p 369.
- (51) Camus, N.; Bris, N. L.; Nuryyeva, S.; Chessé, M.; Esteban-Gómez, D.; Platas-Iglesias, C.; Tripier, R.; Elhabiri, M. Tuning the Copper(II) Coordination Properties of Cyclam by Subtle Chemical Modifications. *Dalton Trans.* **2017**, *46* (34), 11479–11490.
- (52) Sornosa Ten, A.; Humbert, N.; Verdejo, B.; Llinares, J. M.; Elhabiri, M.; Jezierska, J.; Soriano, C.; Kozłowski, H.; Albrecht-Gary, A.-M.; García-España, E. Cu<sup>2+</sup> Coordination Properties of a 2-Pyridine Heptaamine Tripod: Characterization and Binding Mechanism. *Inorg. Chem.* **2009**, *48* (18), 8985–8997.
- (53) Abada, S.; Lecointre, A.; Elhabiri, M.; Charbonnière, L. J. Formation of Very Stable and Selective Cu(II) Complexes with a Non-Macrocyclic Ligand: Can Basicity Rival Pre-Organization? *Dalton Trans.* **2010**, *39* (38), 9055–9062.
- (54) Hathaway, B. J. The Correlation of the Electronic Properties and Stereochemistry of Mononuclear {CuN<sub>4</sub>–6} Chromophores. *J. Chem. Soc., Dalton Trans.* **1972**, No. 12, 1196–1199.
- (55) Wei, N.; Murthy, N. N.; Karlin, K. D. Chemistry of Penta-coordinate [LCuII-Cl]<sup>+</sup> Complexes with Quinoyl Containing Tripodal Tetradentate Ligands L. *Inorg. Chem.* **1994**, *33* (26), 6093–6100.
- (56) Harris, W. R.; Carrano, C. J.; Raymond, K. N. Spectrophotometric Determination of the Proton-Dependent Stability Constant of Ferric Enterobactin. *J. Am. Chem. Soc.* **1979**, *101* (8), 2213–2214.
- (57) Raymond, K. N.; Müller, G.; Matzanke, B. F. Complexation of Iron by Siderophores a Review of Their Solution and Structural Chemistry and Biological Function. In *Topics in Current Chemistry*; Springer: Berlin, Heidelberg, 1984; pp 49–102.
- (58) Wong, E. H.; Weisman, G. R.; Hill, D. C.; Reed, D. P.; Rogers, M. E.; Condon, J. S.; Fagan, M. A.; Calabrese, J. C.; Lam, K.-C.; Guzei, I. A.; et al. Synthesis and Characterization of Cross-Bridged Cyclams and Pendant-Armed Derivatives and Structural Studies of Their Copper(II) Complexes. *J. Am. Chem. Soc.* **2000**, *122* (43), 10561–10572.
- (59) *Méthodes d'Analyses Complexométriques Avec Les Titriplex*; Ed. Merck, Darmstadt.
- (60) Raymond, K. N. *Chemical & Engineering News Archive* **1983**, *61* (49), 4–5.
- (61) Gans, P.; O'Sullivan, B. GLEE, a New Computer Program for Glass Electrode Calibration. *Talanta* **2000**, *51* (1), 33–37.

- (62) Gans, P.; Sabatini, A.; Vacca, A. Investigation of Equilibria in Solution. Determination of Equilibrium Constants with the HYPERQUAD Suite of Programs. *Talanta* **1996**, *43* (10), 1739–1753.
- (63) Gampp, H.; Maeder, M.; Meyer, C. J.; Zuberbühler, A. D. Calculation of Equilibrium Constants from Multiwavelength Spectroscopic Data—II: Mathematical Considerations. *Talanta* **1985**, *32* (2), 95–101.
- (64) Gampp, H.; Maeder, M.; Meyer, C. J.; Zuberbühler, A. D. Calculation of Equilibrium Constants from Multiwavelength Spectroscopic Data—II: 32, 95. *Talanta* **1985**, *32* (4), 257–264.
- (65) Gampp, H.; Maeder, M.; Meyer, C. J.; Zuberbühler, A. D. Calculation of Equilibrium Constants from Multiwavelength Spectroscopic Data—III: Model-Free Analysis of Spectrophotometric and ESR Titrations. *Talanta* **1985**, *32* (12), 1133–1139.
- (66) Gans, P. *Data Fitting in the Chemical Sciences.*; Chichester, 1992; Vol. 105.
- (67) Marquardt, D. W. An Algorithm for Least-Squares Estimation of Nonlinear Parameters. *Journal of the Society for Industrial and Applied Mathematics* **1963**, *11* (2), 431–441.
- (68) Maeder, M.; Zuberbühler, A. D. Nonlinear Least-Squares Fitting of Multivariate Absorption Data. *Analytical Chemistry* **1990**, *62* (20), 2220–2224.
- (69) Stoll, S.; Schweiger, A. EasySpin, a Comprehensive Software Package for Spectral Simulation and Analysis in EPR. *Journal of Magnetic Resonance* **2006**, *178* (1), 42–55.
- (70) Molton, F. Simultispin: A Versatile Graphical User Interface for the Simulation of Solid-State Continuous Wave EPR Spectra. *Magnetic Resonance in Chemistry* **2020**, *58* (8), 718–726.
- (71) Yagi, M.; Arentsen, L.; Shanley, R. M.; Hui, S. K. High-Throughput Multiple-Mouse Imaging with Micro-PET/CT for Whole-Skeleton Assessment. *Physica Medica* **2014**, *30* (7), 849–853.
- (72) Constantinescu, C. C.; Mukherjee, J. Performance Evaluation of an Inveon PET Preclinical Scanner. *Phys. Med. Biol.* **2009**, *54* (9), 2885–2899.
- (73) Gucht, A. V. D.; Zehou, O.; Djelbani-Ahmed, S.; Valeyrie-Allanore, L.; Ortonne, N.; Brugières, P.; Wolkenstein, P.; Luciani, A.; Rahmouni, A.; Sbidian, E.; et al. Metabolic Tumour Burden Measured by 18F-FDG PET/CT Predicts Malignant Transformation in Patients with Neurofibromatosis Type-1. *PLOS ONE* **2016**, *11* (3), e0151809.

## Graphical TOC



**Best of both :** Novel phosphonated pyridine-appended cyclam and cross-bridged cyclam chelators were synthesized, fully characterized, and successfully used *in vivo* as  $^{64}\text{Cu}$ -PET imaging tracers, where they combine the best properties of previously described methylenephosphonate and picolinate pendants.

---